Antenna Allocation and Pricing in Virtualized Massive MIMO Networks via Stackelberg Game

Ye Liu, Mahsa Derakhshani, *Member, IEEE*, Saeedeh Parsaeefard, *Member, IEEE*, Sangarapillai Lambotharan, *Senior Member, IEEE*, and Kai-Kit Wong, *Fellow, IEEE*

***Abstract*— We study a resource allocation problem for the uplink of a virtualized massive multiple-input multiple-output system, where the antennas at the base station are priced and virtualized among the service providers (SPs). The mobile network operator (MNO) who owns the infrastructure decides the price per antenna, and a Stackelberg game is formulated for the net profit maximization of the MNO, while the minimum rate requirements of SPs are satisfied. To solve the bi-level optimization problem of the MNO, we first derive the closed-form best responses of the SPs with respect to the pricing strategies of the MNO, such that the problem of the MNO can be reduced to a single-level optimization. Then, via transformations and approximations, we cast the MNO's problem with integer constraints into a signomial geometric program (SGP), and we propose an iterative algorithm based on the successive convex approximation (SCA) to solve the SGP. Simulation results show that the proposed algorithm has performance close to the global optimum. Moreover, the interactions between the MNO and SPs in different scenarios are explored via simulations.**

***Index Terms*— Resource allocation, massive MIMO, Stackelberg games, convex approximation, antenna allocation.**

I. Introduction

A. Motivation

VIRTUALIZATION of the physical resources of cellular networks suggests a business model that can be beneficial to both mobile network operators (MNOs) and service providers (SPs) [1]. On the one hand, the MNO can make a profit from leasing its underutilized network facilities to SPs serving their subscribers. On the other hand, by renting the infrastructure from the MNO, SPs can provide customized services to their subscribers without the need to build and maintain their network facilities, saving a huge amount of capital expenditures for the hardware.

The possibility of implementing a massive number of antennas on a base station (BS) brings a tremendous improvement in the capacity of a cellular network [2]. It has been shown in [3] that massive multiple-input multiple-output (MIMO) systems can reduce the transmission power and increase the spectral efficiency by the factor of the number of antennas at the BS. Moreover, due to the channel hardening effect in massive MIMO systems, simple linear precoders can be employed at a BS to support transmissions towards multiple users' with good performance [3].

However, using a large number of antennas at a BS comes with non-trivial operating cost. The work in [4] shows that over 50% of the power consumption of a typical BS in 2010 is due to the power amplifiers, baseband processors, and RF transceivers. The power consumption due to the above factors would be more significant in a massive MIMO system. Then, in order to maximize the energy-efficiency of a massive MIMO system, the number of allocated antennas for transmission/reception [5] or even the number of mounted antennas [6] should be optimized. Similarly, the cost of power consumption should be taken into consideration when an MNO provides data services for making a profit.

In this work, we propose antenna and power allocation via pricing in a virtualized massive MIMO network. The use of pricing mechanism is particularly suitable for the situation where the MNO has the ability to offer hardware facilities as a service [7]. Specifically, the pricing is modeled by a Stackelberg game, which could reflect interactions between the MNO as the leader and the SPs as the followers. Similar to [8] that different entities merges as one and purchase energy from the electricity market, in the proposed model, an MNO owns a BS with a large number of antennas and is willing to lease the antennas to multiple SPs. Exploiting the acquired resources from the MNO, each SP serves a group of uplink users with certain guaranteed quality of service (QoS). The available resources at the MNO are quantified by the number of antennas [9]. The MNO decides the price per antenna for each SP, and the MNO makes a profit from charging the SPs based on the number of antennas the users in each of the SPs would like to purchase. On the other hand, the MNO needs to cover the cost of using the antennas and the backhaul link, and therefore the MNO must determine

Manuscript received November 24, 2017; revised March 29, 2018; accepted May 31, 2018. Date of publication June 12, 2018; date of current version November 16, 2018. This work has been supported by the Engineering and Physical Science Research Council of the UK, EPSRC, under the grants EP/M015475 and EP/M016005. The associate editor coordinating the review of this paper and approving it for publication was Y. J. Zhang. *(Corresponding author: Sangarapillai Lambotharan.)*

Y. Liu was with the Signal Processing and Networks Research Group, Wolfson School of Mechanical, Electrical and Manufacturing Engineering, Loughborough University, Leicestershire LE11 3TU, U.K. He is now with the Department of Engineering Science, University of Oxford, Oxford OX1 3PJ, U.K. (e-mail: ye.liu@eng.ox.ac.uk).

M. Derakhshani and S. Lambotharan are with the Signal Processing and Networks Research Group, Wolfson School of Mechanical, Electrical and Manufacturing Engineering, Loughborough University, Leicestershire LE11 3TU, U.K. (e-mail: m.derakhshani@lboro.ac.uk; s.lambotharan@lboro.ac.uk).

S. Parsaeefard is with the Iran Telecommunication Research Centre, Communication Technologies Department, Tehran 16846-13114, Iran (e-mail: s.parsaeifard@itrc.ac.ir).

K.-K. Wong is with the Department of Electronic and Electrical Engineering, University College London, London WC1E 6BT, U.K. (e-mail: kai-kit.wong@ucl.ac.uk).

Color versions of one or more of the figures in this paper are available online at http://ieeexplore.ieee.org.

Digital Object Identifier 10.1109/TCOMM.2018.2846574

the prices it charges each SP to ensure that the net profit is maximized.

Applying Stackelberg game to model these interactions, constrained by QoS requirements of SPs, the optimization problem of the MNO (leader) would be a bi-level optimization, which is inherently difficult to solve [10]. To tackle this issue, we analytically derive the closed-form solutions of the followers as functions of the pricing strategies of the leader; then, by replacing followers' best responses in the leader's game, the problem is transformed into a single-level optimization problem. Since the derived closed-form follower solutions are of binary nature, we introduce auxiliary optimization variables and present the leader's problem in a more tractable manner. However, the transformed leader's problem is still mixed-integer and also non-convex. To solve this problem, we apply several transformations and approximations, such that the leader's problem is cast into a signomial geometric program (SGP) with binary variables. We then propose an algorithm that solves N continuous SGPs, where N is a linear function of the size of the system. An iterative algorithm based on the successive convex approximation (SCA) is applied to solve each of the continuous SGPs. Simulation results show that the proposed iterative algorithm returns the net profit of the MNO which is very close to the optimal net profit found by exhaustive search. Also, various scenarios are examined revealing the profitable situations for the MNO.

B. Related Works

Network virtualization in wireless communications along with software-defined networking (SDN) has been identified as a promising solution to accommodate the diverse demand of wireless communications traffic by introducing flexibility in service customization [11]. Moreover, network function virtualization is argued to be an efficient tool to optimize the resource provisioning in 5G networks where multiple radio access technologies coexist [12]. In this type of 5G networks, physical resources in various radio access networks can be abstracted and virtualized based on which system optimization and customized service provisioning can be accomplished [13]. There are several works in the literature proposing resource allocation techniques in virtualized wireless networks, leveraging the synergy between SDN and multi-layer resource management. For example, [14] and [15] focus on how to carry out vertical handover across cellular network and WiFi access points for traffic offloading and user experience improvement, respectively. In [16], the physical-layer resources from different MNOs are virtualized as achievable data rates and a rate allocation optimization problem is studied. Moreover, virtualization for device-to-device communications has been considered in [17]–[19], and virtualization of cellular networks with full-duplex relays is considered in [20]. The combination of content virtualization [21] and network virtualization is considered in [22] and [23], where caching is enabled at the base stations and the mobile terminals.

Wireless network virtualization not only provides an efficient platform to optimize the system performance of today's highly heterogeneous networks but also makes diverse service provisioning possible [24]. On the other hand, the available service comes with a cost to the MNOs and the SPs, and careful treatment on how to charge for the provided services are needed to ensure the benefits of both parties. Most of the above works in wireless virtualized networks address the resource allocation problem by assuming that the price per unit of resource paid by the service-subscribing users is fixed. Such approaches are not able to capture the behavior of the service subscribers under various pricing strategies and are therefore not suitable for studying the resource allocation problems in virtualized networks from the economy point of view.

To address this issue, Stackelberg game theoretic model can be applied such that the entities who own wireless physical or computational resources can optimize their prices based on the demand from the service subscribers. Such models have been considered in cloud computing for computational resource allocations [25], [26], in cognitive radio networks for spectrum trading [27], and in full-duplex relay assisted cellular networks for energy-efficient resource allocation [28]–[30]. In massive-MIMO enabled networks, hierarchical evolutionary game and combinatorial auction have been adopted to address the antenna allocation problem in [31] and [32], respectively. However, the cost for operating a large number of antennas is not considered in [31], [32]. Reference [33] investigates antenna and subcarrier allocation for energy efficiency maximization in a virtualized massive-MIMO single-cell network, but the interactions between SPs and MNOs from an economic perspective is not studied.

In this work, we study the joint resource allocation and service provisioning pricing problem in massive-MIMO enabled wireless virtualized networks, where the antennas are priced for the profit maximization of the MNO, and the cost of operating the antennas are taken into account. We adopt a Stackelberg game approach, which allows us to study the behaviors of the data service subscribers in a virtualized massive MIMO network and the optimal pricing strategy of the MNO who provides the infrastructure. Through extensive analyses, we characterize the behaviors of the users belonging to different SPs under various pricing strategies. Based on simulation studies, we identify the conflicts between the MNO and the SPs, and we discuss the scenarios which are beneficial to the MNO and the SPs.

C. Organization

The rest of this paper is organized as follows. Section II presents the system model and formulates the Stackelberg game for the resource allocation problem. Section III derives the closed-form solutions of the followers in the Stackelberg game and formulates the single-level leader problem. Section IV details the proposed algorithm for solving the leader problem. Section V provides the numerical studies for the iterative algorithm and the behaviors of the leader and the followers in the Stackelberg game. Finally, Section VI draws the conclusion.

II. System Model

Consider a cellular network where an MNO owns a BS which is equipped with M antennas. There are G SPs in

the network; each SP provides uplink service to a group of users by renting the hardware from the MNO. Denote $\mathcal{G} \triangleq \{1, 2, \ldots, G\}$ as the index set for the SPs, where SP g serves N_g users whose indices are contained in the set $\mathcal{N}_g \triangleq \{1, 2, \ldots, N_g\}$.

Let $\mathbf{h}_{n,g}$ be the M-by-1 channel coefficient vector between the BS and the n-th user in SP g. We model the channel coefficient as $\mathbf{h}_{n,g} = \sqrt{d_{n,g}}\mathbf{g}_{n,g}$, where $d_{n,g}$ is the large-scale fading gain between the BS and the n-th user in SP g which is assumed to be the same for all antennas, and $\mathbf{g}_{n,g}$ denotes the vector of small-scale fading coefficients. The elements in $\mathbf{g}_{n,g}$ are assumed to be mutually independent. Also, $\mathbf{g}_{n,g}$ and $\mathbf{g}_{n',g}$ are assumed to be independent for $n \neq n'$.

Denote $M_{n,g}$ as the number of antennas allocated to the n-th user in SP g, and $\mathbf{h}_{n,g}$ the corresponding $M_{n,g}$-by-1 channel coefficients from the BS. Due to the vision that massive-MIMO is a key enabler of the next generation cellular network, we focus on the situation where the system operates at the massive-MIMO region, where $M_{n,g} \geq M_{\min}$ and $M_{\min}$ is sufficiently large. Then, from the law of large numbers, we have $\frac{1}{M_{n,g}}\mathbf{h}_{n,g}^{\dagger}\mathbf{h}_{n',g'} \approx 0$ for $n' \neq n$ or $g' \neq g$. Also, we have $\frac{1}{M_{n,g}}\mathbf{h}_{n,g}^{\dagger}\mathbf{h}_{n,g} \approx d_{n,g}$. With perfect channel state information, the achievable uplink data rate of the n-th user in SP g using maximal-ratio combining (MRC) is [3]

$$R_{n,g} = \ln(1 + P_{n,g}M_{n,g}d_{n,g}), \tag{1}$$

where $P_{n,g}$ is the transmission power of the user and the noise power is normalized to one.[1]

The MNO charges SP g for the number of antennas allocated to its users with a price of c_g, such that c_g is the charge per-antenna for SP g. Consequently, the total charge of SP g can be computed as $c_g \sum_{n_g \in \mathcal{N}_g} M_{n,g}$. Accordingly, the charge incurred to SP g due to user n is $c_g M_{n,g}$. Denote θ_g as the willingness to pay for SP g, where higher θ_g indicates that the users of the SP g are willing to pay more for the same level of services [35]. By adapting the widely used linear utility model [32], [36], the utility of the n-th user in SP g is defined as the difference between its gain from receiving the data service and the induced cost, i.e.,

$$U_{n,g}(P_{n,g}, M_{n,g}) \triangleq \theta_g R_{n,g} - w_g P_{n,g} - c_g M_{n,g}, \tag{2}$$

where w_g is a power weight on the transmission power level, which is considered for power conservation. Note that although the transmission power budget constraint for a user is not explicitly defined, we show later that the utility definition in (2) imposes a maximum transmission power for a user implicitly.

Due to a finite number of antennas mounted at the BS, the number of available antennas for allocation to any user is limited as

$$M_{n,g} \leq M, \quad \forall n, \ \forall g. \tag{3}$$

[1]As indicated in [34] that the rate expression for the downlink scenario depends on the number of simultaneously served users. As a result, the game theoretic analysis for the uplink, to be presented later, is significantly different from the downlink. Therefore, we leave the downlink scenario as a future work.

Furthermore, in order to avoid the situation in which a user is forced to pay for the antennas while receiving no data service, the following constraint on the number of allocated antennas to the n-th user in SP g is imposed, i.e.,

$$M_{n,g} \geq M_{\min} \cdot \mathbb{1}(P_{n,g}), \tag{4}$$

where $\mathbb{1}(\cdot)$ is the indicator function which is defined as $\mathbb{1}(x) \triangleq 0$ if $x = 0$ and $\mathbb{1}(x) \triangleq x$ if $x >= 0$. The physical meaning of (4) is that a user has the option not to purchase any antenna, if the user decides not to transmit any data.

At the MNO side, the cost induced to provide the uplink services needs to be considered for net profit maximization. Since the antennas at the BS can be used to process the received signals from multiple users, the cost due to the operation of antennas is proportional to the maximum number of allocated antennas. Therefore, according to the power consumption model in [6], we define the cost of the MNO as

$$f_{\text{MNO}}^{\text{cost}} \triangleq q_1 \cdot \max_{n \in \mathcal{N}_g, g \in \mathcal{G}} \{M_{n,g}\} + q_2 \cdot \sum_{g \in \mathcal{G}} \sum_{n \in \mathcal{N}_g} R_{n,g}, \tag{5}$$

where the first part of (5) quantifies the cost that comes from the received signal processing at the BS, the second part of (5) quantifies the cost that comes from demodulation, channel decoding, and data transfer to the core network via the backhaul, and q_1 and q_2 are the costs per antenna and per unit of data rate, respectively. Define $\hat{M}$ as an auxiliary variable that serves as the upper bound on the number of allocated antennas to the users. The cost function of the MNO can be equivalently written as

$$f_{\text{MNO}}^{\text{cost}} = q_1 \hat{M} + q_2 \sum_{g \in \mathcal{G}} \sum_{n \in \mathcal{N}_g} R_{n,g}, \quad \hat{M} \geq M_{n,g}, \ \forall n, \ \forall g. \tag{6}$$

For the sake of fairness and service customization of the SPs, the MNO ensures that the total achieved uplink data rate of SP g is no less than a positive value $R_g^{\min}$ [33], i.e.,

$$\sum_{n \in \mathcal{N}_g} R_{n,g} \geq R_g^{\min}, \quad g \in \mathcal{G}. \tag{7}$$

Since the MNO decides the price per antenna which affects the net profit of itself and the utilities of the users, it is convenient to use the Stackelberg game to model the profit maximization and user utility maximization problem. In the proposed Stackelberg game framework, the MNO is the leader, and the SPs are the followers. The net profit maximization problem for the leader and utility maximization problems for the followers can be formulated as

Leader (MNO):

$$\underset{\{c_g | g \in \mathcal{G}\}}{\text{maximize}} \ \sum\nolimits_{g \in \mathcal{G}} \left(c_g \sum\nolimits_{n \in \mathcal{N}_g} M_{n,g} \right) - f_{\text{MNO}}^{\text{cost}}, \tag{8a}$$

$$\text{subject to} \ \sum\nolimits_{n \in \mathcal{N}_g} R_{n,g} \geq R_g^{\min}, \quad \forall g \in \mathcal{G}, \tag{8b}$$

$$\hat{M} \leq M, \tag{8c}$$

$$M_{n,g} \leq \hat{M}, \quad \forall n, \ \forall g, \tag{8d}$$

Follower g (SP g):

$$\underset{\{P_{n,g},M_{n,g}|n\in\mathcal{N}_g\}}{\text{maximize}} \sum\nolimits_{n\in\mathcal{N}_g} U_{n,g}, \tag{9a}$$

$$\text{subject to } P_{n,g}\geq 0, \quad n\in\mathcal{N}_g, \tag{9b}$$

$$M_{n,g}\geq M_{\min}\cdot\mathbb{1}(P_{n,g}), \quad n\in\mathcal{N}_g, \tag{9c}$$

$$M_{n,g}\in\mathbb{Z}^+, \quad n\in\mathcal{N}_g. \tag{9d}$$

We can see that the leader's problem is a bi-level optimization problem because the leader's problem formulation depends on the output of the followers' optimization problems.

The formulated Stackelberg game can be solved by first finding the subgame perfect equilibria of the followers' games, i.e., the closed-form solutions to the follower games. Then, the leader's problem can be reduced to a single-level optimization problem by substituting the followers' solutions into the leader's problem. Next, we devote Section III to finding the solutions of the follower games and Section IV-C to solving the leader game in single-level form.

III. Subgame Perfect Equilibria Analysis and the Single-Level Leader's Problem Formulation

In this section, we analyze the subgame perfect equilibria of the followers' games and provide closed-form solutions of the followers. In other words, we find the best responses of the followers for a given strategy of the leader in terms of c_g. Then, we present the formulation of the leader optimization problem in single-level form.

A. Closed-Form Solution of a Follower

The optimization problem (9) is a mixed integer programming since $M_{n,g}$ are restricted to integer values. To reduce the complexity of solving the Stackelberg game, we relax the constraint in (9d) such that $M_{n,g}$ can take real positive values.[2] To find the global maximum of this constrained problem, we first study the properties of critical points (CPs) of $U_{n,g}$ and then explore the global maximum within the feasible region.

1) Critical Points of $U_{n,g}$: Setting the first order partial derivatives of $U_{n,g}$ with respect to (w.r.t.) $P_{n,g}$ and $M_{n,g}$ to zero, we have

$$\frac{\partial U_{n,g}}{\partial P_{n,g}}0 \Rightarrow P_{n,g}=\frac{\theta_g}{w_g}-\frac{1}{M_{n,g}d_{n,g}}, \tag{10}$$

$$\frac{\partial U_{n,g}}{\partial M_{n,g}}=0 \Rightarrow M_{n,g}=\frac{\theta_g}{c_g}-\frac{1}{P_{n,g}d_{n,g}}. \tag{11}$$

To find the CPs of $U_{n,g}$ (when they exist), we search for the intersection points of the curves $\frac{\partial U_{n,g}}{\partial P_{n,g}}=0$ and $\frac{\partial U_{n,g}}{\partial M_{n,g}}=0$. The values of $P_{n,g}$ at the CPs of $U_{n,g}$ can be found by substituting (11) into (10), which results in

$$-c_g P_{n,g}^2+\theta_g P_{n,g}-c_g d_{n,g}^{-1}=0, \tag{12}$$

[2]The relaxation of $M_{n,g}$ should not have much effect on the optimal solution much, because the values of θ_g, w_g, and c_g can be relatively small compared to the value of $M_{n,g}$. Notice that it is the ratios among θ_g, w_g, and c_g that affects the optimization problem. Moreover, the simulation results in Fig. 2 supports our claim.

The solution of (12) can be found as

$$P_{n,g}=\frac{\theta_g\pm\sqrt{\alpha_{n,g}}}{2w_g}. \tag{13}$$

when $\alpha_{n,g}>0$, where

$$\alpha_{n,g}\triangleq\theta_g^2-c_g\hat{d}_{n,g}^{-1},\ \hat{d}_{n,g}\triangleq\frac{d_{n,g}}{4w_g}. \tag{14}$$

Substituting (13) into (11), the two CPs of $U_{n,g}$ are

$$\textbf{CP-1: } \left(P_{n,g}=\frac{\theta_g+\sqrt{\alpha_{n,g}}}{2w_g}, M_{n,g}=\frac{\theta_g+\sqrt{\alpha_{n,g}}}{2c_g}\right),$$

$$\textbf{CP-2: } \left(P_{n,g}=\frac{\theta_g-\sqrt{\alpha_{n,g}}}{2w_g}, M_{n,g}=\frac{\theta_g-\sqrt{\alpha_{n,g}}}{2c_g}\right).$$

When $\alpha_{n,g}=0$, the only CP is

$$\textbf{CP-3: } \left(P_{n,g}=\frac{\theta_g}{2w_g}, M_{n,g}=\frac{\theta_g}{2c_g}\right).$$

Moreover, when $\alpha_{n,g}<0$, no CP exists for the function $U_{n,g}$. The next theorem shows the properties of CP-1 and CP-2 when $\alpha_{n,g}>0$.

Theorem 1: Given that $\alpha_{n,g}>0$, CP-1 is a local maximum and CP-2 is a saddle point, where $U_{n,g}$(CP-1) $\geq U_{n,g}$(CP-2).

Proof: See Appendix A. ∎

2) Best Responses of Followers: We now identify the global maximum of $U_{n,g}$, i.e., the best responses of the followers. Since the existence of local optima affects the behavior of $U_{n,g}$, we divide the discussions into the following three parts

a. No CP exists, i.e., $\alpha_{n,g}<0$ or $c_g>\theta_g^2\hat{d}_{n,g}$,
b. CP-3 exists, i.e., $\alpha_{n,g}=0$ or $c_g=\theta_g^2\hat{d}_{n,g}$, and
c. CP-1 and CP-2 exist, i.e., $\alpha_{n,g}>0$ or $c_g<\theta_g^2\hat{d}_{n,g}$.

Note that the existence of the CPs depends on the value of c_g. More specifically, CPs exist if the price of SP g is small enough.

Before analyzing the optimal response of a user, we reveal in the following lemma the optimal $P_{n,g}$ that maximizes $U_{n,g}$ when fixing $M_{n,g}$ and vice versa. The lemma is important for searching for the global maximum of $U_{n,g}$ in various scenarios where CPs may or may not exist.

Lemma 1: Fixing $M_{n,g}$, the maximum of $U_{n,g}$ happens at $P_{n,g}=\frac{\theta_g}{w_g}-\frac{1}{M_{n,g}d_{n,g}}$ such that $\frac{\partial U_{n,g}}{\partial P_{n,g}}=0$. Also, when $P_{n,g}$ is fixed, the maximum of $U_{n,g}$ happens at $M_{n,g}=\frac{\theta_g}{c_g}-\frac{1}{P_{n,g}d_{n,g}}$ such that $\frac{\partial U_{n,g}}{\partial M_{n,g}}=0$.

Proof: See Appendix B. ∎

We now find the global maximum of $U_{n,g}$ when $c_g>\theta_g^2\hat{d}_{n,g}$. In this case, $U_{n,g}$ has no CP, which means that the curves $\frac{\partial U_{n,g}}{\partial P_{n,g}}=0$ and $\frac{\partial U_{n,g}}{\partial M_{n,g}}=0$ do not intersect with each other. Let

$$\hat{w}_{n,g}\triangleq\frac{w_g}{M_{\min}d_{n,g}} \tag{15}$$

be the normalized weight for the transmission power of the n-th user in SP g. The next theorem shows the global maximum of $U_{n,g}$ when $c_g>\theta_g^2\hat{d}_{n,g}$.

Theorem 2: When $c_g > \theta_g^2 \hat{d}_{n,g}$, the maximum of $U_{n,g}$ is obtained at the boundary point

1) ***B-1:*** $(P_{n,g} = 0, M_{n,g} = 0)$, *when* $\hat{w}_{n,g} \geq \theta_g$,
2) ***B-2:*** $\left(P_{n,g} = \frac{\theta_g}{w_g} - \frac{1}{M_{min} d_{n,g}}, M_{n,g} = M_{min}\right)$, *when* $\hat{w}_{n,g} < \theta_g$.

Proof: See Appendix C. ∎

From Theorem 2, it would be advantageous for the leader to set a large price when $\hat{w}_{n,g} < \theta_g$ since a user would always purchase some antennas for a large c_g and the payment from the user would then be very large. However, such advantage can be easily counteracted if SP g either increases w_g or decreases θ_g such that $\hat{w}_{n,g} \geq \theta_g$ for all users in the SP. In that case, no user from SP g will be willing to subscribe any service, and the leader will not be able to take any advantage. In the sequel, we assume that $\hat{w}_{n,g} \geq \theta_g$ to avoid the leader from taking the unfair advantage as described above.

Next, we state the global maximum of $U_{n,g}$ when $c_g = \theta_g^2 \hat{d}_{n,g}$ such that CP-3 exists.

Theorem 3: When $c_g = \theta_g^2 \hat{d}_{n,g}$ and $\hat{w}_{n,g} \geq \theta_g$, the maximum of $U_{n,g}$ happens at B-1.

Proof: See Appendix D. ∎

Theorem 3 together with Theorem 2 imply that the n-th user in SP g will always prefer to transmit at zero power and purchase no data service when $c_g \geq \theta_g^2 \hat{d}_{n,g}$ and $\hat{w}_g \geq \theta_g$.

Next, we discuss the feasibility condition of CP-1 and the user's best response when $c_g < \theta_g^2 \hat{d}_{n,g}$, where we know from previous discussions that CP-1 exists when $c_g < \theta_g^2 \hat{d}_{n,g}$.

Theorem 4: When $c_g < \theta_g^2 \hat{d}_{n,g}$ and $\hat{w}_g \geq \theta_g$, CP-1 is feasible. Also, there exists a threshold price $\varrho_{n,g} \in (0, \theta_g^2 \hat{d}_{n,g})$ such that leftmargin=5mm

1) *the n-th user in SP g plays CP-1 as the best response, if $c_g < \varrho_{n,g}$, and,*
2) *B-1 is the best response of the same user, if $c_g \in [\varrho_{n,g}, \theta_g^2 \hat{d}_{n,g})$.*

Moreover, the threshold price $\varrho_{n,g}$ is the unique solution of

$$U_{n,g}(\textbf{CP-1}) = \theta_g \log(2\theta_g \frac{\theta_g + \sqrt{\alpha_{n,g}}}{c_g \hat{d}_{n,g}^{-1}}) - (\theta_g + \sqrt{\alpha_{n,g}}) = 0, \tag{16}$$

and $\varrho_{n,g}$ can be found by the bisection method.

Proof: See Appendix E. ∎

Theorem 4 implies that when $c_g < \theta_g^2 \hat{d}_{n,g}$, the n-th user in SP g might purchase more antennas than $M_{\min}$. This is because, when $c_g < \theta_g^2 \hat{d}_{n,g}$, CP-1 can be the best response of the n-th user in SP g. Since $\frac{\theta_g + \sqrt{\alpha_{n,g}}}{2c_g}$ (the optimal $M_{n,g}$ in CP-1) is a decreasing function of c_g and $\lim_{c_g \to 0^+} \frac{\theta_g + \sqrt{\alpha_{n,g}}}{2c_g} = +\infty$, the n-th user in SP g would purchase many antennas if the leader sets c_g very small. Moreover, although the optimal power at CP-1 $\frac{\theta_g + \sqrt{\alpha_{n,g}}}{2w_g}$ is a decreasing function of c_g, the n-th user in SP g always transmits at a positive power since $\frac{\theta_g + \sqrt{\alpha_{n,g}}}{2w_g} > \frac{\theta_g}{2w_g}$ when $c_g < \theta_g^2 \hat{d}_{n,g}$. Thus, given that there is sufficient number of antennas, the leader is able to satisfy a high $R_g^{\min}$ by reducing c_g when CP-1 exists and is feasible.

Summarizing the results in Theorems 2, 3, and 4, we obtain the best response of a user for any non-negative c_g and any positive w_g as follows.

Corollary 1: For $\hat{w}_g \geq \theta_g$, the best response of the n-th user in SP g is CP-1 when $c_g < \varrho_{n,g}$ and is B-1 when $c_g \geq \varrho_{n,g}$. The threshold price $\varrho_{n,g}$ is the unique solution of (16)*.*

Remark 1: Although no constraint has been imposed on the maximum transmission power for each user, it is evident that the maximum transmission power of the n-th user in SP g is $\frac{\theta_g}{w_g}$, which will happen only if $U_{n,g}$ is maximized at CP-1 and c_g approaches zero. In other words, a suitable w_g can be chosen to ensure that the power budget of a user is respected.

Remark 2: The optimal $M_{n,g}$ is always a decreasing function of c_g. This can be explained by the fact that, when $c_g \leq \theta_g^2 \hat{d}_{n,g}$, $M_{n,g}^* = \frac{\theta_g + \sqrt{\alpha_{n,g}}}{2c_g}$ which is a decreasing function of c_g and always larger than $M_{\min}$. When $c_g > \theta^2 \hat{d}_{n,g}$, $M_{n,g}^* = 0$. This means that the followers would purchase more antennas if c_g decreases.

Remark 3: For SP g, there exists an upper bound $c_g^{\max}$ and a lower bound $c_g^{\min}$ on c_g such that the leader's problem is feasible if $c_g \in [c_g^{\min}, c_g^{\max}]$. To see this, the rate constraint in (8b) will be violated if c_g is too large because no user in SP g would purchase any antenna, and the antenna allocation constraints in (8c) and (8d) will be violated if c_g is too small because $\lim_{c_g \to 0^+} \frac{\theta_g + \sqrt{\alpha_{n,g}}}{2c_g} = +\infty$, i.e., a user purchases a large number of antennas for small c_g. The values of $c_g^{\max}$ and $c_g^{\min}$ can be found by bisection methods.

B. Single-Level Formulation of the Leader's Game

In this section, we present the single-level formulation of the leader problem based on the best responses of the followers. From Corollary 1, the best response of a user is of binary nature, i.e., either CP-1 or B-1. To be able to reflect the possibilities of the best responses in the leader problem formulation, we introduce binary auxiliary variables, i.e., $l_{n,g}$, as the indicators for the best response of the n-th user in SP g such that

1) $l_{n,g} = 1$ when CP-1 is the best response, and,
2) $l_{n,g} = 0$ when B-1 is the best response.

Then, the optimal transmission power and the number of allocated antennas of the n-th user in SP g can be written as

$$P_{n,g}^{\text{best}} \triangleq \frac{\theta_g + \sqrt{\alpha_{n,g}}}{2w_g} l_{n,g}, \tag{17}$$

$$M_{n,g}^{\text{best}} \triangleq \frac{\theta_g + \sqrt{\alpha_{n,g}}}{2c_g} l_{n,g}. \tag{18}$$

From Corollary 1, the value of $l_{n,g}$ depends on c_g and $\varrho_{n,g}$. The next lemma defines a set of constraints on $l_{n,g}$ which reflects the necessary conditions on best responses.

Lemma 2: The following constraints

$$l_{n,g} \leq \varrho_{n,g} c_g^{-1}, \tag{19a}$$

$$(l_{n,g} + c_g \varrho_{n,g}^{-1})^{-1} \leq 1, \tag{19b}$$

$$l_{n,g} \in \{0, 1\}, \tag{19c}$$

ensure that: $l_{n,g} = 1$ *when* $c_g < \varrho_{n,g}$*;* $l_{n,g} = 0$ *when* $c_g > \varrho_{n,g}$*; Either* $l_{n,g} = 1$ *or* $l_{n,g} = 0$ *when* $c_g = \varrho_{n,g}$.

Proof: The lemma can be proved by checking feasible $l_{n,g}$ and c_g values. ∎

With the new auxiliary variables (i.e., $l_{n,g}$, $P_{n,g}^{\text{best}}$, and $M_{n,g}^{\text{best}}$) and the new constraints (i.e., (19)), the leader problem (8) can be transformed into

$$\underset{\substack{c_g, R_{n,g}, l_{n,g}, \\ P_{n,g}^{\text{best}}, M_{n,g}^{\text{best}}, \hat{M}}}{\text{minimize}} \sum_{g\in\mathcal{G}} \sum_{n\in\mathcal{N}_g} \left(q_2\ R_{n,g} - c_g M_{n,g}^{\text{best}}\right) + q_1 \hat{M}, \quad (20a)$$

$$\text{subject to}\ \ e^{R_{n,g}} = 1 + P_{n,g}^{\text{best}} M_{n,g}^{\text{best}} d_{n,g},\ \forall n,\ \forall g, \quad (20b)$$

$$R_g^{\min} \cdot \left(\sum\nolimits_{n\in\mathcal{N}_g} R_{n,g}\right)^{-1} \le 1,\ g \in \mathcal{G}, \quad (20c)$$

$$M_{n,g}^{\text{best}} \le \hat{M},\ \forall n,\ \forall g, \quad (20d)$$

$$c_g \in [c_g^{\min}, c_g^{\max}],\ \forall g, \quad (20e)$$

$$(8c),\ (17),\ (18),\ \text{and}\ (19),$$

where (20b) is the equivalent transformations of (1).

The problem in (20) falls into the category of mixed-integer nonlinear program (MINLP) [37]. A general approach to a MINLP is to use the branch-and-bound method whose complexity in the worst case can be as high as exhaustive search, i.e., the number of solved subproblems can be an exponential function of the number of variables [38]. MINLPs which are non-convex after the integer relaxation are even more difficult to solve because the complexity of solving any problem instances during the branching process can be very high. Obtaining the optimal solution of (20) is then very challenging because the problem is non-convex even after the binary relaxation.

In the next section, we propose an algorithm to solve (20) that searches through selected subproblems of (20). In this approach, the number of solved subproblems is only a linear function of the size of the system, and each subproblem contains only continuous variables. We then propose an efficient iterative algorithm that solves the non-convex subproblems of (20). The performance of the algorithm is very close to that obtained by the exhaustive search as demonstrated in the simulation studies.

IV. Proposed Algorithm for the Leader's Game

We propose an algorithm for solving (20) with affordable complexity. We first show that the optimal solution of (20) can be found by solving $\prod_{g=1}^{G} N_g$ subproblems of (20) without binary variables. Then, we propose an algorithm that explores in a reduced search space, such that at most $\sum_{g=1}^{G} N_g - G + 1$ out of the $\prod_{g=1}^{G} N_g$ subproblems of (20) are solved. Subsequently, we propose an efficient iterative algorithm that finds an optimal solution for each subproblem.

A. Binary Relaxations

The relationship among c_g, $l_{n,g}$, and $\varrho_{n,g}$ in (19) suggests that $l_{n,g}$ takes fixed values when c_g belongs to certain ranges defined by $\varrho_{n,g}$. The next lemma describes $\varrho_{n,g}$ as a function of $d_{n,g}$, which facilitates the determination of $l_{n,g}$ values in different ranges of c_g.

Lemma 3: $\varrho_{n,g}$ *is an increasing function of* $d_{n,g}$.

Proof: See Appendix F. ∎

With out loss of generality, assume that the user indices of each SP are arranged such that $d_{i,g} \le d_{j,g}, \forall i < j \in \mathcal{N}_g$, $\forall g$ where $i, j \in \mathcal{N}_g$. From Lemma 3 and Theorem 4, we can infer the best responses of all users in SP g when $c_g \in [\varrho_{n',g}, \varrho_{n'+1,g}]$. Specifically, $l_{n,g} = 1$ for all $n \in \mathcal{N}_g$ such that $n \ge n'$ and $l_{n,g} = 0$ for users with indices $n < n'$.

The above observation can be leveraged to remove the binary variables. Suppose that $\varrho_{0,g} \triangleq 0\ \forall g$. The following constraint

$$\text{Con}(n'_g, g) : \varrho_{n'_g,g} \le c_g \le \varrho_{n'_g+1,g} \quad (21)$$

is equivalent to

$$l_{n,g} = \begin{cases} 0,\ \forall n < n'_g \\ 1,\ \forall n \ge n'_g \end{cases} \quad (22)$$

where $n'_g \in \{0\} \cup \mathcal{N}_g \setminus \max\{\mathcal{N}_g\}$, $\mathcal{A}\setminus\mathcal{B}$ gives the elements in $\mathcal{A}$ that are not in $\mathcal{B}$, $g \in \mathcal{G}$, and $\max\{\mathcal{N}_g\}$ returns the largest element in the set $\mathcal{N}_g$. Consequently, by adding $\text{Con}(n'_g, g)$ for all SPs, we can remove the binary variables $l_{n,g}$ and obtain a continuous subproblem of (20) as

$$\underset{\substack{c_g, R_{n,g}, \\ P_{n,g}^{\text{best}}, M_{n,g}^{\text{best}}, \hat{M}}}{\text{minimize}} \sum_{g\in\mathcal{G}} \sum_{n\in\mathcal{A}_g(n'_g)} \left(q_2\ R_{n,g} - c_g M_{n,g}^{\text{best}}\right) + q_1 \hat{M}, \quad (23a)$$

$$\text{subject to}\ e^{R_{n,g}} = 1 + P_{n,g}^{\text{best}} M_{n,g}^{\text{best}} d_{n,g},\quad \forall n \in \mathcal{A}_g(n'_g),\ \forall g, \quad (23b)$$

$$P_{n,g}^{\text{best}} = 0,\ \forall n \in \mathcal{N}_g \setminus \mathcal{A}_g(n'_g),\quad \forall g \in \mathcal{G}, \quad (23c)$$

$$M_{n,g}^{\text{best}} = 0,\ \forall n \in \mathcal{N}_g \setminus \mathcal{A}_g(n'_g),\quad \forall g \in \mathcal{G}, \quad (23d)$$

$$R_g^{\min} \cdot \left(\sum\nolimits_{n\in\mathcal{A}_g(n'_g)} R_{n,g}\right)^{-1} \le 1,\quad \forall g \in \mathcal{G}, \quad (23e)$$

$$P_{n,g}^{\text{best}} = \frac{\theta_g + \sqrt{\alpha_{n,g}}}{2w_g},\ \forall n \in \mathcal{A}_g(n'_g),\quad \forall g \in \mathcal{G}, \quad (23f)$$

$$M_{n,g}^{\text{best}} = \frac{\theta_g + \sqrt{\alpha_{n,g}}}{2c_g},\ \forall n \in \mathcal{A}_g(n'_g),\quad \forall g \in \mathcal{G}, \quad (23g)$$

$$\text{Con}(n'_g, g):\ \varrho_{n'_g,g} \le c_g \le \varrho_{n'_g+1,g},\quad \forall g \in \mathcal{G}, \quad (23h)$$

$$(20e), (20d),\ \text{and}\ (8c),$$

where $\mathcal{A}_g(n'_g) \triangleq \{n'_g + 1, n'_g + 2, \ldots, N_g\}$ for a given $n'_g \in \{0\} \cup \mathcal{N}_g \setminus \max\{\mathcal{N}_g\}$. Note that $\mathcal{A}_g(n'_g)$ represents the active user set of SP g when the constraint $\text{Con}(n'_g, g)$ is added, where an active user plays CP-1 as its best response and an inactive user plays B-1 as its best response.

Note that there are N_g possible constraints of the kind $\text{Con}(n'_g, g)$ for SP g. Considering all combinations, we have in total $\prod_{g=1}^{G} N_g$ subproblems in the form of (23). To obtain the optimal solution of (20), the exhaustive approach is to solve all $\prod_{g=1}^{G} N_g$ subproblems of (20). However, the complexity of solving all $\prod_{g=1}^{G} N_g$ subproblems becomes prohibitive as a subproblem of (20) is non-convex and the number of subproblems grows quickly with the number of users.

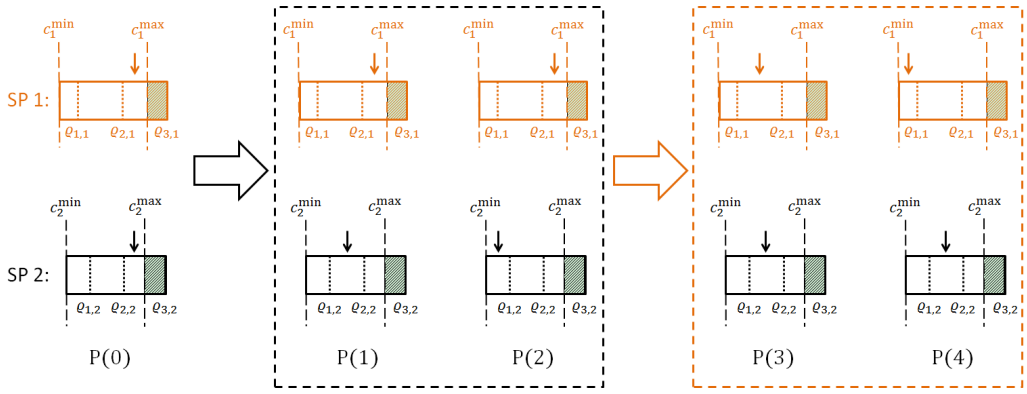

Fig. 1. Illustration of the proposed search algorithm. In this example, there are two SPs, where each SP serves 3 users. The users of SP 1 are labeled as 1, 2, and 3, and the users of SP 2 are labeled in a similar way. The pointers represent the constraints $\text{Con}(n'_g, g)$ in (23), e.g., the two pointers on the far left means that $\text{Con}(2,1)$ and $\text{Con}(2,2)$ are included in the initial instance of (23), i.e., $\text{P}(0)$. Prices in the shaded areas are not feasible.

B. Search Algorithm With Linear Complexity

We now propose a search algorithm that drastically reduces the number of subproblems of (20) needed to be solved. The proposed search algorithm is motivated by the following observation: Suppose SP g purchases M' antennas, the cost induced to the leader due to the operation of antennas will remain fixed as long as no other SP purchases more than M'. This allows the leader to explore the possibility of increasing the net profit by encouraging other SPs, who currently purchased fewer antennas than M', to purchase more by decreasing the price.

Inspired by the above observation, we propose a search procedure where only $\sum_{g=1}^{G} N_g - G + 1$ problems of the kind in (23) need to be solved. We illustrate the proposed algorithm in Fig. 1 for two SPs, where both SPs 1 serve 3 users. The algorithm contains the following steps:

1) *Starting with the highest feasible price ranges:* We start the pricing optimization by constraining the price of each SP to the largest interval defined by the threshold prices, where the interval contains price values that are feasible. In this step, the number of antennas allocated to each SP would be in the lowest range possible.
   Example: In Fig. 1, $c_2 \geq \varrho_{3,2}$ is not feasible for satisfying the rate requirement of SP 2. Therefore, we start by solving (23) with $c_1 \in [\varrho_{2,1}, \varrho_{3,1}]$ and $c_2 \in [\varrho_{2,2}, \varrho_{3,2}]$. In other words, the constraints in (23h) are $\text{Con}(2,1)$ and $\text{Con}(2,2)$ (see the first instance on the left of Fig. 1). We denote this instance of (23h) as the *initial instance* $\text{P}(0)$.
2) *Decreasing the price range for one SP:* In this step, we adjust the price range for one SP while fixing the price ranges for the other SPs and solve the corresponding sub-problem (23). In other words, the algorithm explores the possibility to sell more antennas to an SP for profit maximization by searching in a reduced range of prices. We do so for each SP, where we start from the SP that purchases the least number of antennas in $\text{P}(0)$, proceed to the next SP that purchases the second least number of antennas in $\text{P}(0)$, and stop at the SP that purchases the most number of antennas in $\text{P}(0)$.
   Example Continued: Referring to Fig. 1, suppose after solving $\text{P}(0)$, SP 1 purchases more antennas than SP 2. Then, we solve another two instances of (23) which we denote respectively as $\text{P}(1)$ and $\text{P}(2)$. In $\text{P}(1)$ and $\text{P}(2)$, the price range constraint for SP 2 in (23h) are respectively $\text{Con}(1,2)$ and $\text{Con}(0,2)$, and the same constraint for SP 1 is $\text{Con}(2,1)$.
   Now, suppose the leader gains the largest net profit in $\text{P}(1)$. Then, we solve another two instances of (23) which are $\text{P}(3)$ and $\text{P}(4)$, where the price range constraints for SP 1 in $\text{P}(3)$ and $\text{P}(4)$ are respectively $\text{Con}(1,1)$ and $\text{Con}(0,1)$, and the price range of SP 2 is $\text{Con}(1,2)$. Suppose $\text{P}(3)$ maximizes the net profit of leader among $\text{P}(1)$, $\text{P}(3)$, and $\text{P}(4)$. Then, we return the solution of $\text{P}(3)$ as the output of the search algorithm.

To calculate the number of subproblems that the proposed search algorithm needs to solve, observe that the first step solves one subproblem. Then, in the second step, for SP g, at most $N_g - 1$ subproblems are solved when $[c_g^{\min}, c_g^{\max}]$ includes all threshold prices $\{\varrho_{n,g} | n \in \mathcal{N}_g\}$. Therefore, the total number of subproblems that needs to be solved by the proposed search algorithm is upper-bounded by $\sum_{g=1}^{G} N_g - G + 1$.

Next, we propose an iterative algorithm that efficiently solves the non-convex problem (23).

C. An Iterative Algorithm for the Leader's Subproblems

We now propose an iterative algorithm for solving a problem instance in (23). We first show that (23) can be cast into an SGP, where solving an SGP is NP-hard [39]. Then, we apply the SCA method, where (23) is solved by solving a series of GPs. Note that a GP can be transformed into a convex problem which can be efficiently solved.

1) Preliminaries on Solving an SGP: Let $\mathbf{x} \triangleq [x_0, x_1, \ldots, x_N]$ be the variables to be optimized. An SGP can be written in the following form

$$\textbf{SGP}: \underset{\mathbf{x}}{\text{minimize}} \quad x_0, \tag{24a}$$

$$\text{subject to} \quad \frac{f_k(\mathbf{x})}{f'_k(\mathbf{x})} \leq 1, \quad k \in \mathcal{K}_1, \tag{24b}$$

$$\frac{f_k(\mathbf{x})}{f'_k(\mathbf{x})} = 1, \quad k \in \mathcal{K}_2, \tag{24c}$$

where $f_k(\mathbf{x}) \triangleq \sum_j \gamma_{j,k} \prod_i x_i^{\delta_{i,j,k}}$ and $f'_k(\mathbf{x}) \triangleq \sum_j \gamma'_{j,k} \prod_i x_i^{\delta'_{i,j,k}}$ are posynomials, $\gamma_{j,k} > 0$, $\gamma'_{j,k} > 0$, $\delta_{i,j,k}$ and $\delta'_{i,j,k}$ are real numbers, and $\mathcal{K}_1$ and $\mathcal{K}_2$ are two disjoint index sets.

Due to its NP-hardness, solving an SGP optimally in general leads to high computational complexity. On the other hand, it has been shown that SCA can be applied where a Karush-Khun-Tucker (KKT) point of the SGP can be obtained [40]. In the SCA, a GP approximation of the SGP is obtained at the t-th iteration, where the GP approximation is based on the solution of the GP in the last iteration $\mathbf{x}(t)$, and the first GP approximation is performed based on an initial point $\mathbf{x}(0)$. A solution to the SGP is then found by solving a series of GPs, where a GP can be transformed into a convex problem which can be solved efficiently by off-the-shelf optimization toolboxes such as MOSEK.

To approximate the SGP in (24) at the t-th iteration using a GP, a two-step transformation can be carried out. As the first step, define $\{s_k(t)|k \in \mathcal{K}_2\}$ as the auxiliary variables, the problem (24) can be equivalently transformed into

$$\underset{\mathbf{x},\{s_k|k\in\mathcal{K}_2\}}{\text{minimize}} \; x_0(t) + \sum_{k\in\mathcal{K}_2} \mu_k(t) s_k(t), \tag{25a}$$

$$\text{subject to} \; \frac{f_k(\mathbf{x}(t))}{f'_k(\mathbf{x}(t))} \leq 1, \quad k \in \mathcal{K}_1 \cup \mathcal{K}_2, \tag{25b}$$

$$\frac{s_k(t)^{-1} f'_k(\mathbf{x}(t))}{f_k(\mathbf{x}(t))} \leq 1, \quad k \in \mathcal{K}_2, \tag{25c}$$

$$s_k(t) \geq 1, \quad k \in \mathcal{K}_2, \tag{25d}$$

when $s_k(t) = 1$ for all $k \in \mathcal{K}_2$, where $\{\mu_k(t)|k \in \mathcal{K}_2\}$ are chosen as positive and increasing functions of t such that $s_k(t)$ is forced to take small values as t increases [40].

As a second step of the GP approximation, the denominators of the constraints (25b) and (25c) are replaced by monomials using the arithmetic-geometric mean approximation (AGMA), such that (25b) and (25c) become upper bound constraints on posynomials which can be admitted by a GP. Let $f'_k(\mathbf{x}(t)) = \sum_j \tilde{f}_{k,j}(\mathbf{x}(t))$, where $\tilde{f}_{k,j}$ are monomials, the AGMA suggests that

$$\sum_j \tilde{f}_{k,j}(\mathbf{x}(t)) \geq \prod_j \left(\frac{\tilde{f}_{k,j}(\mathbf{x}(t))}{b_{k,j}(t)} \right)^{b_{k,j}(t)}, \tag{26}$$

where $b_{k,j}(t) \triangleq \frac{\tilde{f}_{k,j}(\mathbf{x}(t-1))}{f'_k(\mathbf{x}(t-1))}$ and $\mathbf{x}(t-1)$ is obtained from the last iteration [40]. Then, the constraints in (25b) can be approximated as

$$f_k(\mathbf{x}(t)) \cdot \prod_j \left(\frac{\tilde{f}_{k,j}(\mathbf{x}(t))}{b_{k,j}(t)} \right)^{-b_{k,j}(t)} \leq 1, \quad k \in \mathcal{K}_1 \cup \mathcal{K}_2. \tag{27}$$

After the aforementioned transformations, a GP approximation of the original SGP is obtained at the t-th iteration. The iterative algorithm for solving an SGP takes the following steps

S-1 Set $t = 0$. Initialize $\mathbf{x}(t)$ and $\mu_k(t)$.

S-2 Set $t = t + 1$. Set $\mu_k(t)$ such that $\mu_k(t) \geq \mu_k(t-1)$. Find the GP approximation of the SGP based on (25) and (26). Then, solve the resultant GP.

S-3 Repeat step 2 until some stopping criterion is met. Return $\mathbf{x}(t)$ as the solution to the SGP.

The convergence of the SCA towards a KKT point is established in [40], and we omit the corresponding discussion here for simplicity.

2) Leader Sub-Problem as an SGP: The problem in (23) takes a form which is similar to an SGP. We discuss some transformations required to model the leader game as an SGP.

To cast the objective function of (23) into SGP, we first add a sufficiently large constant E to (23a) such that (23a) is guaranteed to be positive. Then, by introducing an auxiliary variable z, (23a) becomes equivalent to the minimization of z subject to the following constraint

$$\sum_{g\in\mathcal{G}} \sum_{n\in\mathcal{A}_g(n'_g)} \left(q_2 \; R_{n,g} - c_g M_{n,g}^{\text{best}}\right) + q_1 \hat{M} + E \leq z$$
$$\Rightarrow \frac{\sum_{g\in\mathcal{G}} \sum_{n\in\mathcal{A}_g(n'_g)} (q_2 \; R_{n,g}) + q_1 \hat{M} + E}{\sum_{g\in\mathcal{G}} \sum_{n'\in\mathcal{A}_g(n'_g)} c_g M_{n,g}^{\text{best}} + z} \leq 1, \tag{28}$$

In addition, we approximate the term $e^{R_{n,g}}$ in (20b) using a truncated Taylor series as

$$e^{R_{n,g}} = \sum_{i=0}^{+\infty} \frac{R_{n,g}^i}{i!} \approx \sum_{i=0}^{Q} \frac{R_{n,g}^i}{i!}, \tag{29}$$

where Q is a positive integer which is sufficiently large such that the approximation is accurate. Then, the problem (23) can be rewritten as the following SGP

$$\underset{c_g, y_{n,g}, P_{n,g}^{\text{best}}, M_{n,g}^{\text{best}}, \hat{M}, z}{\text{minimize}} \; z, \tag{30a}$$

$$\text{subject to} \; \sum_{i=1}^{Q} \frac{R_{n,g}^i}{i! \cdot P_{n,g}^{\text{best}} M_{n,g}^{\text{best}} d_{n,g}} = 1,$$
$$n \in \mathcal{A}_g(n'_g), \quad g \in \mathcal{G},$$
$$\text{(8c), (20d), (20e), and (28),}$$
$$\text{(23e)} - \text{(23h)}, \tag{30b}$$

where (30b) is the transformation of (20b) after the approximation in (29).

3) GP Approximation of the Leader's Problem: The constraints in (8c), (20e), (20d), and (23h) are readily admissible to a GP, while all other constraints in (30) must be approximated before being admissible by a GP.

We now apply the two-step transformation introduced in Section IV-C.1 to obtain the GP approximation of (30), where the iteration index t is appended to all variables to indicate there status at the t-th iteration of the SCA. Let $\{s_{j,g,n}(t)|j \in \{1,2,3\}, n \in \mathcal{A}_g(n'_g), g \in \mathcal{G}\}$ be the auxiliary variables and let $\{\mu_{j,g,n}(t)|j \in \{1,2,3\}, n \in \mathcal{A}_g(n'_g), g \in \mathcal{G}\}$ be the

corresponding weighting functions. Moreover, let

$$\varphi_{j,g,n}(t) \triangleq \begin{cases} \sum_{i=1}^{Q} \dfrac{R_{n,g}^{i}(t)}{i! \cdot P_{n,g}^{\text{best}}(t) M_{n,g}^{\text{best}}(t) d_{n,g}}, & j=1, \\ \theta_g^{-1} w_g P_{n,g}^{\text{best}} + \theta_g^{-1} d_{n,g}^{-1} c_g {P_{n,g}^{\text{best}}}^{-1}, & j=2, \\ \theta_g^{-1} c_g M_{n,g}^{\text{best}} + \theta_g^{-1} d_{n,g}^{-1} w_g {M_{n,g}^{\text{best}}}^{-1}, & j=3, \end{cases} \tag{31}$$

such that the functions in $\{\varphi_{j,g,n}(t) | j \in \{1,2,3\}\}$ represent the left hand side of the constraints in (30b), (23f), and (23g). At the t-th iteration, (30) can be transformed into

$$\underset{\substack{y_{n,g}(t), P_{n,g}^{\text{best}}(t), \\ M_{n,g}^{\text{best}}(t), c_g(t), \hat{M}(t), \\ z(t), s_{j,g,n}(t)}}{\text{minimize}} \quad z(t) + \sum_{g \in \mathcal{G}} \sum_{n \in \mathcal{A}_g(n'_g)} \sum_{j=1}^{3} \mu_{j,g,n}(t) s_{j,g,n}(t), \tag{32a}$$

subject to (8c), (20d), (20e), (28), (23e), and (23h)

$$\varphi_{j,g,n}(t) \leq 1, \quad j \in \{1,2,3\}, \\ n \in \mathcal{A}_g(n'_g), \quad g \in \mathcal{G}, \tag{32b}$$

$$s_{j,g,n}^{-1}(t) \cdot \varphi_{j,g,n}^{-1}(t) \leq 1, \quad j \in \{1,2,3\}, \\ n \in \mathcal{A}_g(n'_g), \quad g \in \mathcal{G}, \tag{32c}$$

$$s_{j,g,n}(t) \geq 1, \quad j \in \{1,2,3\}, \\ n \in \mathcal{A}_g(n'_g), \quad g \in \mathcal{G}, \tag{32d}$$

so that the equality constraints in (23f), (23g), and (30b) are transformed into inequality constraints. Then, to obtain the GP approximation of (32), AGMA is applied to the denominators of the left hand sides of the constraints in (23e), (28), and (32c). The details of the AGMA approximations are omitted for simplicity.

4) Complexity: The interior-point method can be used to solve a GP and it is widely used in off-the-shelf solvers such as MOSEK. The interior-point method is an iterative algorithm that gradually approaches the global optimal point of a convex problem. One implementation of the interior-point method is the barrier method [41], where the number of iterations required can be found as $\mathcal{O}(\log(\kappa))$ where κ is the number of inequality constraints in the convex problem. The formulation in (32) contains at most $\kappa = 6\sum_{g=1}^{G} N_g + G + 5$ inequality constraints. Therefore, the interior-point method can solve the GP approximation of (32) in $\mathcal{O}(\log(\sum_{g=1}^{G} N_g))$ iterations. We resort to simulation studies to demonstrate the number of GPs solved using the SCA.

V. Simulation Results

We evaluate the proposed algorithm in the following simulation setup. Specifically, the BS is located at the origin of the Cartesian coordinate and users are randomly distributed in the coverage area of the BS. With path-loss exponent equal to 3.7, $d_{n,g} = \iota_{n,g}^{-3.7}$, where $\iota_{n,g} \in [2,5]$ denotes the normalized distance between the BS and the n-th user in SP g. M_{min} is set to 20, and R_g^{min} is set to 1 for all SPs. For an accurate approximation in (29), we set $Q = 15$. The simulation results are averaged over 500 randomly generated topologies in terms of user locations.

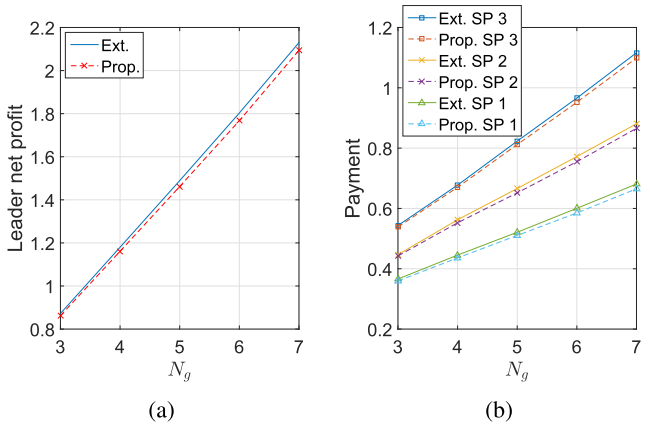

Fig. 2. Leader net profit and the payment from each SP when varying the number of users in each SP, where $G = 3$ and the numbers of users in all SPs are the same. $w_g = 0.5$ for all SPs, $\theta_1 = 0.3$, $\theta_2 = 0.35$, and $\theta_3 = 0.4$. M is set to 600. In the legends, "Ext." denotes the results from the exhaustive search, and "Prop." denotes the results from the proposed algorithm.

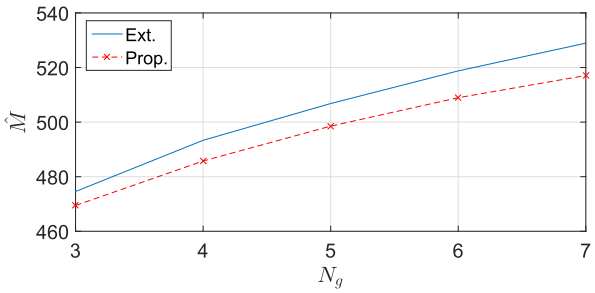

Fig. 3. Number of used antennas at the BS, where the system parameters of the figure are the same as those of Fig. 2.

Fig. 2 compares the proposed algorithm against the exhaustive search method, where $G = 3$. The exhaustive search is done by identifying the feasible price regions $[c_g^{\text{min}}, c_g^{\text{max}}]$ for each of the three SPs, taking 200 uniform samples from each of the feasible price regions, and testing all combinations of the price samples for the three SPs. q_1 and q_2 are both set to 0.001's. The results from Fig. 2 demonstrates that the proposed algorithm is able to let the leader achieves a net profit very close to the maximum possible net profit. The same figures also reveal that the leader can make more profit when the number of users in the SPs increases, because the payment from an SP increases as the number of users increases. Moreover, SP 3 pays the most among the three SPs, because the willingness to pay of SP 3 is the highest.

Fig. 3 shows the number of allocated antennas at the BS and the prices for each SP using the same system settings as those in Fig. 2. Observe from Fig. 3 that the proposed algorithm correctly reflects the trend of $\hat{M}$ against the number of users in each SP, and the proposed algorithm returns the value $\hat{M}$ that is very close to that returned by the exhaustive search. An implication of the results from Fig. 3 is that the leader finds it more profitable to sell more antennas to

TABLE I
AVERAGE NUMBER OF ITERATIONS USED FOR THE SCA

N_g	3	4	5	6	7
# Iter.	10.57	10.80	11.03	11.25	11.46

the followers even if it means that the price per antenna needs to be reduced, because there are more users to make payment.

Table I shows the average number of iterations used for the SCA algorithm described in S-1 to S-3 under the scenario in Fig. 2. For the SCA, we initialize $\mu_{j,g,n}(0) = 0.01$ for all j, g, and n. We increase $\mu_{j,g,n}(t)$ by $\upsilon(t)$ at iteration t, where $\upsilon(0) = 0.01$ at the beginning of the SCA. We increase the step size υ by 9 times (i.e., $\upsilon(t) = 10\upsilon(t-1)$) if the maximum decrease from $s_{j,g,n}(t-1)$ to $s_{j,g,n}(t)$ is less than one percent, where the maximum is taken over all the indices of $s_{j,g,n}$. We stop the SCA if either the maximum of $s_{j,g,n}(t)$ is less than $1+10^{-10}$ or υ has been updated 20 times. By such a step-size updating rule, we find out that the largest value of $s_{j,g,n}(t)$ when the algorithm terminates is 1.0016, which suggests that the algorithm terminates at a point that is very close to an KKT point of the leader's problem in (20). The results in Table I shows that the number of iterations for the SCA increases as the size of the system increases, but the increase on the number of iterations of the SCA is quite marginal with respect to N_g. This suggests that the complexity of the SCA does not increase significantly regarding N_g.

When the number of SPs, i.e., G, in the system increases, we can see from Fig. 4a that the net profit of the leader increases as the number of SPs increases. The reason can be explained in two-fold. On one hand, the increase of SPs allows the leader to receive more payment. On the other hand, because antennas can be reused by users from different SPs, the cost in terms of antennas can be "shared" by the SPs. Therefore, as depicted in Fig. 4b, the leader is able to encourage the followers to purchase more antennas when the number of SPs increases.

We now examine the effect of power weight w_g. Fig. 4c shows that the net profit of the leader decreases as w_g increases. From the best response analysis of the followers, we can see that the users reduce their transmission power when w_g increases. This can force the leader to allocate more antennas, as seen in Fig. 4d, for the purpose of satisfying the QoS constraints of the SPs but not for increasing the net profit.

Fig. 5 show how service customization regarding QoS requirement alters the decision of the leader, where we set $R_1^{\min} = R_2^{\min} = R_3^{\min}$. Also, we examine the obtained service of each SP regarding the total achieved rate of the users in each SP when the distance distributions of the SPs are different. Specifically, the user distance distribution of SP 1 remains unchanged, while $\iota_{n,g} \in [2.6, 2.8]$ for SP 2 and $\iota_{n,g} \in [3.4, 3.6]$ for SP 3.

We can see from Fig. 5c that as $R_g^{\min}$ increases, the leader needs to reduce the price per antenna so that more antennas are purchased by the SPs. On the other hand, Fig. 5b shows

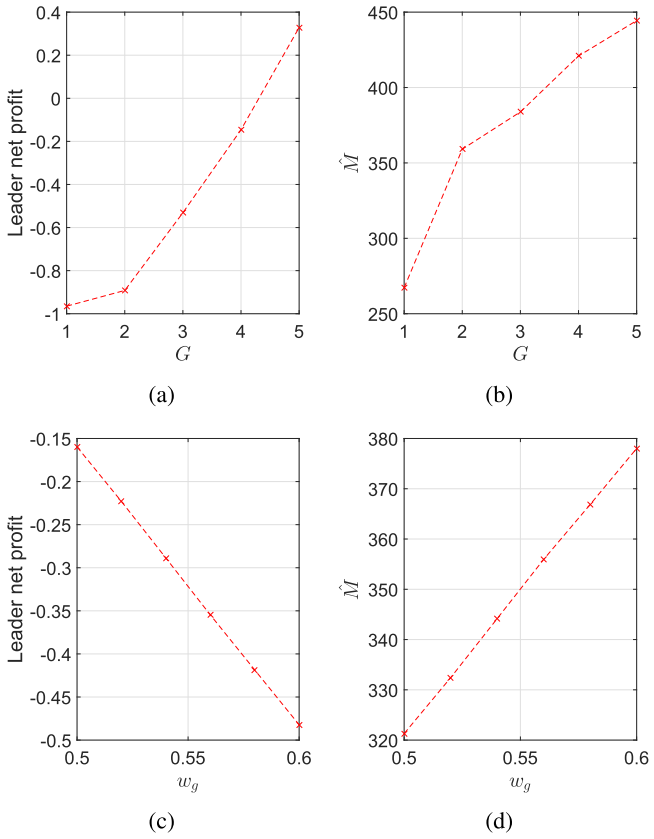

Fig. 4. Leader net profit and the number of used antennas at the BS for different number of SPs and different weighting factors as obtained using the proposed algorithm. For Fig. 4a and Fig. 4b, $N_g = 4$, $w_g = 0.6$, and $\theta_g = 0.4$ for all SPs. $q_1 = q_2 = 0.005$. For Fig. 4c and Fig. 4d, $N_g = 4$, $\theta_g = 0.4$, $q_1 = q_2 = 0.005$, and all SPs use the same w_g. M is set to 600.

that SP 3 achieves the same rate as $R_3^{\min}$ when $R_3^{\min} = 7$. This indicates that the leader struggles to meet the QoS requirement of SP 3 when $R_3^{\min}$ becomes large, and for that the leader needs to reduce c_3 and may harvest less profit from SP 3. Due to the fact that the users of SP 2 have good channel gains, it is relatively easy for the leader to satisfy the QoS requirement of SP 2. As a result, the leader has more choices on setting c_2. The leader then exploits this convenience by setting c_2 such that SP 2 purchases roughly the same amount of antennas as SP 1 does, where the number of antennas sold to SP 2 are much larger than the amount needed for achieving $R_2^{\min}$ (see Fig. 5b). By doing so, the leader harvests the most payment from SP 2 among all SPs. Although the achieved rate of SP 1 is larger than $R_1^{\min}$, it is harder for the leader to harvest profit from SP 1 as demonstrated in Fig. 5d, because the distance distribution of the users in SP 1 has large variance and the leader's profit can be low when it is hard to ensure the QoS requirement of SP 1, i.e., when most of the users of SP 1 happen to be located far away from the BS.

Summarizing the above results, we find out that the MNO can make profit if it serves more SPs with more users who are more willing to pay for the service, and the profit of the MNO will drop if the users are more conservative on spending their

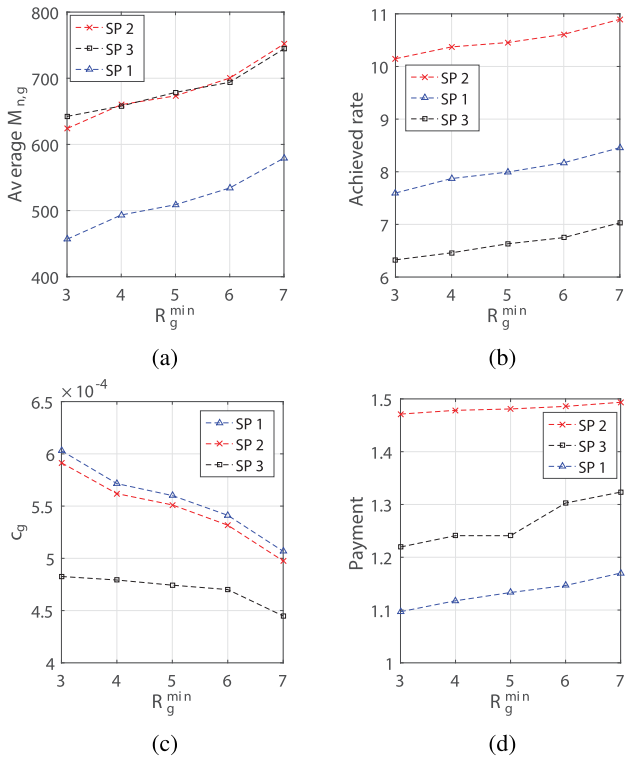

Fig. 5. Average allocated antennas per user, average achieved rate of each SP, price, and payment of each SP for different $R_g^{\min}$ as obtained using the proposed algorithm, where $R_1^{\min} = R_2^{\min} = R_3^{\min}$. $w_1 = w_2 = w_3 = 0.5$, and $\theta_1 = \theta_2 = \theta_3 = 0.4$.

transmission power. Also, the leader can receive more payment if an SPs serves users that are located closer to the BS.

VI. Conclusion

We have studied a virtualized massive MIMO network which provides uplink services to multiple SPs. We have formulated the service provisioning and resource allocation problem as a Stackelberg game, where we have derived the closed-form expressions of the uplink users' best responses w.r.t. the price issued by the MNO. Based on the closed-form solutions of the users and some transformations, we have formulated the leader problem as an discrete SGP with binary variables. Due to the NP-hardness of solving the binary SGP optimally, we have developed an algorithm that solves a linear number (w.r.t. to the size of the system) of continuous SGPs, and we have implemented an iterative algorithm for solving each of the continuous SGPs that converges to a KKT point. Simulation results have demonstrated the close-to-optimal performance of the proposed algorithm. Also, various simulation scenarios have been studied to demonstrate the interactions between MNO and the SPs, revealing the profitable situations for the MNO.

The current work considers the pricing of antennas only during the service provision by the MNO. Given that the antennas are just one type of the resources that an MNO possesses, more comprehensive studies on pricing other resources, e.g., frequency spectrum, can be considered in future extensions. Moreover, a competitive scenario among the SPs that mimics the real market can be another important future direction.

Appendix A
Proof of Theorem 1

The second order partial derivatives of $U_{n,g}$ w.r.t. $P_{n,g}$ and $M_{n,g}$ can be found as

$$\frac{\partial^2 U_{n,g}}{\partial P_{n,g}^2} = -\frac{\theta_g M_{n,g}^2 d_{n,g}^2}{(1+P_{n,g}M_{n,g}d_{n,g})^2},$$

$$\frac{\partial^2 U_{n,g}}{\partial M_{n,g}^2} = -\frac{\theta_g P_{n,g}^2 d_{n,g}^2}{(1+P_{n,g}M_{n,g}d_{n,g})^2},$$

$$\frac{\partial^2 U_{n,g}}{\partial P_{n,g}\partial M_{n,g}} = \frac{\partial^2 U_{n,g}}{\partial M_{n,g}\partial P_{n,g}} \frac{\theta_g d_{n,g}}{(1+P_{n,g}M_{n,g}d_{n,g})^2}. \quad (33)$$

From (33), we have

$$\Phi(P_{n,g}, M_{n,g}) \triangleq \frac{\partial^2 U_{n,g}}{\partial P_{n,g}^2}\frac{\partial^2 U_{n,g}}{\partial M_{n,g}^2} - \left(\frac{\partial^2 U_{n,g}}{\partial P_{n,g}\partial M_{n,g}}\right)^2 = \frac{\theta_g^2 P_{n,g}^2 M_{n,g}^2 d_{n,g}^2 - 1}{(1+P_{n,g}M_{n,g}d_{n,g})^4} d_{n,g}^2. \quad (34)$$

For the critical point CP-1, one can easily check that $\frac{\partial^2 U_{n,g}}{\partial P_{n,g}^2}(\text{CP-1}) < 0$ and $\Phi(\text{CP-1}) > 0$, which suggest that CP-1 is a local maximum [42]. Also, for the critical point CP-2, one can find that $\Phi(\text{CP-2}) < 0$, which suggests that CP-2 is a saddle point [42].

To verify if $U_{n,g}(\text{CP-1}) \geq U_{n,g}(\text{CP-2})$, we examine the following expression

$$U_{n,g}(\text{CP-1}) - U_{n,g}(\text{CP-2}) = \theta_g \ln\left(\frac{\theta_g + \sqrt{\alpha_{n,g}}}{\theta_g - \sqrt{\alpha_{n,g}}}\right) - 2\sqrt{\alpha_{n,g}}. \quad (35)$$

The derivative of (35) w.r.t. $\alpha_{n,g}$ can be found as $\frac{\sqrt{\alpha_{n,g}}}{\theta_g^2 - \alpha_{n,g}}$ which is positive when $\alpha_{n,g} \in [0, \theta_g]$. Notice that the interval $[0, \theta_g]$ includes all possible values that $\alpha_{n,g}$ can take. Thus, (35) is minimized when $\alpha_{n,g} \to 0$. Consequently, $U_{n,g}(\text{CP-1}) \geq U_{n,g}(\text{CP-2})$ is true because

$$\lim_{\alpha_{n,g}\to 0^+} \left\{\theta_g \ln\left(\frac{\theta_g + \sqrt{\alpha_{n,g}}}{\theta_g - \sqrt{\alpha_{n,g}}}\right) - 2\sqrt{\alpha_{n,g}}\right\} = 0. \quad (36)$$

Appendix B
Proof of Lemma 1

When $M_{n,g}$ is fixed and $P_{n,g}$ is the only variable of $U_{n,g}$, the critical point $P_{n,g} = \frac{\theta_g}{w_g} - \frac{1}{M_{n,g}d_{n,g}}$ is the global maximum because $\frac{\partial^2 U_{n,g}}{\partial P_{n,g}^2} < 0$ (see (33)). Similarly, when $P_{n,g}$ is fixed, the critical point $M_{n,g} = \frac{\theta_g}{c_g} - \frac{1}{P_{n,g}d_{n,g}}$ is the global maximum because $\frac{\partial^2 U_{n,g}}{\partial M_{n,g}^2} < 0$ (see (33)).

APPENDIX C
PROOF OF THEOREM 2

Suppose N_0 is a feasible point on the curve $\frac{\partial U_{n,g}}{\partial M_{n,g}} = 0$, we search for the global maximum from N_0. Let $f_P(\mathrm{N}_0)$ and $f_M(\mathrm{N}_0)$ represent the transmission power of the n-th user in SP g and the number of antennas allocated to the same user at point N_0, respectively. From Lemma 1 and basic geometry (see Fig. 6a), if we fix $M_{n,g}$ to $f_M(\mathrm{N}_0)$, then $U_{n,g}$ increases if we decrease $P_{n,g}$ from $f_P(\mathrm{N}_0)$ until we reach either $\frac{\partial U_{n,g}}{\partial P_{n,g}} = 0$ or $P_{n,g} = 0$, where we must stop decreasing $P_{n,g}$ beyond $P_{n,g} = 0$ because of the feasibility issue. Denote the stopping point as N_1.

To further improve $U_{n,g}$, due to similar reasons, we can fix $P_{n,g}$ and decrease $M_{n,g}$. We can have the following three different cases

1) $f_P(\mathrm{N}_1) > 0$ and $f_M(\mathrm{N}_1) > M_{\min}$: We can improve $U_{n,g}$ by decreasing $M_{n,g}$ until we hit either $\frac{\partial U_{n,g}}{\partial M_{n,g}} = 0$ or $M_{n,g} = M_{\min}$, which ever happens first. Denote the stopping point as N_2. Because $f_P(\mathrm{N}_2) > 0$, we can decrease $P_{n,g}$ from the point N_2 to further improve $U_{n,g}$.
2) $f_P(\mathrm{N}_1) > 0$ and $f_M(\mathrm{N}_1) = M_{\min}$: We cannot improve $U_{n,g}$ by further decreasing $P_{n,g}$ because N_1 lies on the curve $\frac{\partial U_{n,g}}{\partial P_{n,g}} = 0$. Also, we cannot improve $U_{n,g}$ by further decreasing $M_{n,g}$ because of feasibility issue. Note that in this case, $f_P(\mathrm{N}_1) = \frac{\theta_g}{w_g} - \frac{1}{M_{\min} d_{n,g}}$, and $f_P(\mathrm{N}_1) > 0$ implies that $\frac{w_g}{M_{\min} d_{n,g}} < \theta_g$. The search stops; call the stopping point as B-2.
3) $f_P(\mathrm{N}_1) = 0$ and $f_M(\mathrm{N}_1) \geq M_{\min}$: We can improve $U_{n,g}$ by decreasing $M_{n,g}$ from $f_M(\mathrm{N}_1)$ to 0. The search is stopped; let us call the stopping point as B-1.

We now show that the above procedure always converges when being carried out iteratively. Let N_i be the point that is found in the i-th iteration. Then, for any positive integer i, we have $f_P(\mathrm{N}_{2i}) \leq f_P(\mathrm{N}_{2i-1}) = f_P(\mathrm{N}_{2i-2})$, $f_M(\mathrm{N}_{2i}) = f_M(\mathrm{N}_{2i-1}) \leq f_M(\mathrm{N}_{2i-2})$, and $U_{n,g}(\mathrm{N}_i) \geq U_{n,g}(\mathrm{N}_{i-1})$, where $f_P(\mathrm{N}_{2i}) = \max\{0, \frac{1}{w_g} - \frac{1}{f_M(\mathrm{N}_{2i-1}) \cdot d_{n,g}}\}$ and $f_M(\mathrm{N}_{2i}) = \max\{M_{\min} \cdot \mathbb{1}(f_P(\mathrm{N}_{2i-2})), \frac{1}{c_g} - \frac{1}{f_P(\mathrm{N}_{2i-2}) \cdot d_{n,g}}\}$. Also, following the aforementioned iterative procedure, for any positive integer i, we have

$$\begin{aligned} &f_P(\mathrm{N}_i) \geq 0, f_M(\mathrm{N}_i) \geq M_{\min} \cdot \mathbb{1}(f_P(\mathrm{N}_i)), \\ &f_P(\mathrm{N}_i) \geq \frac{1}{w_g} - \frac{1}{f_M(\mathrm{N}_i) \cdot d_{n,g}}, \\ &f_M(\mathrm{N}_i) \geq \frac{1}{c_g} - \frac{1}{f_P(\mathrm{N}_i) \cdot d_{n,g}}. \end{aligned} \tag{37}$$

Because both $f_P(\mathrm{N}_i)$ and $f_M(\mathrm{N}_i)$ are decreasing functions of i, by repeating the above steps, we will reach the boundary of the region defined by (37) such that neither $f_P(\mathrm{N}_i)$ nor $f_M(\mathrm{N}_i)$ can be further reduced.

It can be concluded that either of the stopping points, i.e., B-1 or B-2, is indeed the global maximum when $\alpha_{n,g} < 0$ because

1) The choice of N_0 on the curve $\frac{\partial U_{n,g}}{\partial P_{n,g}} = 0$ is an arbitrary feasible point, and,

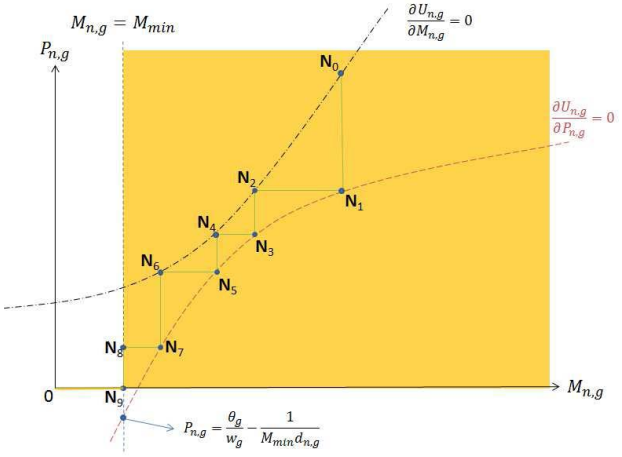

(a)

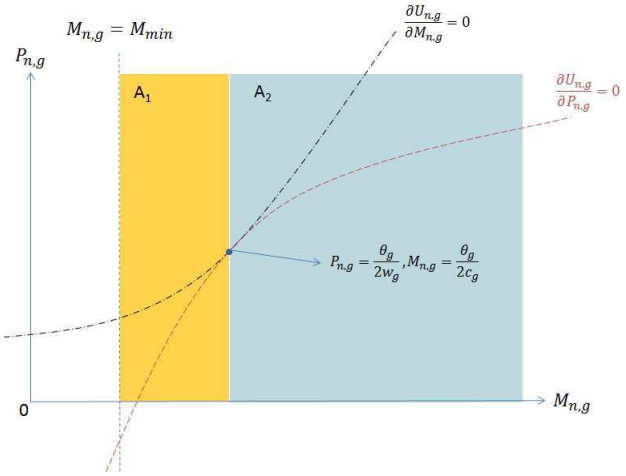

(b)

Fig. 6. Illustration of the search for the global maximum of $U_{n,g}$, where feasible regions of $U_{n,g}$ are shaded. (a) The case when $\alpha_{n,g} < 0$ and $\hat{w}_g > \theta_g$. The proof of Theorem 2 shows that $U_{n,g}(\mathrm{N}_0) \leq U_{n,g}(\mathrm{N}_1) \leq U_{n,g}(\mathrm{N}_2) \leq \ldots \leq U_{n,g}(\mathrm{N}_9) \leq U_{n,g}(0,0)$. Note that the line from (0,0) to N_9 is also feasible. (b) the case when $\alpha_{n,g} = 0$ and $\hat{w}_g > \theta_g$. A1 and A2 respectively label the feasible regions $M_{n,g} \in [M_{\min}, \frac{\theta_g}{2c_g}]$ and $M_{n,g} > \frac{\theta_g}{2c_g}$.

2) Suppose we start with any feasible arbitrary point N', then from Lemma 1, $U_{n,g}(\mathrm{N}_0) \geq U_{n,g}(\mathrm{N}')$, where $f_M(\mathrm{N}_0) = f_M(\mathrm{N}')$ and N_0 is on the curve $\frac{\partial U_{n,g}}{\partial P_{n,g}} = 0$.

APPENDIX D
PROOF OF THEOREM 3

Given that $c_g = \theta_g^2 \hat{d}_{n,g}$ and $\hat{w}_{n,g} \geq \theta_g$, we have

$$\frac{\theta_g}{2c_g} = \frac{2w_g}{\theta_g d_{n,g}} = \frac{2\hat{w}_g M_{\min}}{\theta_g} \geq 2M_{\min} > M_{\min}. \tag{38}$$

We now search for the global maximum using the similar approach in Appendix C. If we randomly select a feasible point in the region $M_{n,g} < \frac{\theta_g}{2c_g}$ and repeat the procedure in the proof of Theorem 2, we find out that the point B-1 results in the largest $U_{n,g}$ (see Fig. 6b). On the other hand, if we randomly select a feasible point in the region $M_{n,g} \geq \frac{\theta_g}{2c_g}$

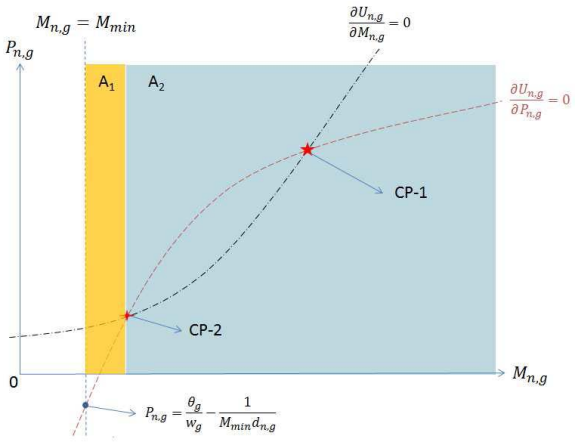

Fig. 7. Illustration of the search for the global maximum of $U_{n,g}$, where $\alpha_{n,g} < 0$ and $\hat{w}_g > \theta_g$. The shaded area is the feasible region of $U_{n,g}$.

and repeat the procedure in the proof of Theorem 2, it can be concluded that CP-3 results in the largest $U_{n,g}$. We must then compare B-1 and CP-3 in order to find the global maximum. To this end, we have

$$\begin{aligned} U_{n,g}(\text{CP-3}) - U_{n,g}(\text{B-1}) &= \theta_g \log(1 + \frac{\theta_g^2}{c_g \hat{d}_g^{-1}}) - \theta_g \\ &= \theta_g \log(2) - \theta_g < 0, \end{aligned} \quad (39)$$

which indicates that B-1 is the global optimal point.

Appendix E
Proof of Theorem 4

For the feasibility of CP-1, since $\frac{1+\sqrt{\alpha_{n,g}}}{2w_g} \geq 0$ when $c_g < \theta_g^2 \hat{d}_{n,g}$, we only need to show that

$$\frac{\theta_g + \sqrt{\alpha_{n,g}}}{2c_g} \geq M_{\min} \Leftrightarrow \sqrt{\alpha_{n,g}} \geq 2c_g M_{\min} - \theta_g. \quad (40)$$

To this end, first, the conditions $c_g < \theta_g^2 \hat{d}_{n,g}$ and $\hat{w}_g > \theta_g$ implies that $c_g < \frac{\theta_g^2}{4\ w_g d_{n,g}^{-1}}$ and $\frac{\theta_g M_{\min}}{2 w_g d_{n,g}^{-1}} < \frac{1}{2}$, respectively. These two conditions then suggest that

$$2c_g M_{\min} - \theta_g < \theta_g \cdot \left(\frac{\theta_g M_{\min}}{2 w_g d_{n,g}^{-1}} - 1 \right) < 0. \quad (41)$$

Then, (40) is true given (41), which suggests that CP-1 is feasible.

We now search for the global optimal point of $U_{n,g}$. Starting from an arbitrary feasible point, we would stop at either CP-1 or B-1 if we use the same searching approach as the one in Appendix B (Fig. 7 shows the graph that facilitates the search when CP-2 is feasible). To find out the global optimal point, we investigate the following difference, i.e.,

$$\begin{aligned} &U_{n,g}(\text{CP-1}) - U_{n,g}(\text{B-1}) \\ &\quad = U_{n,g}(\text{CP-1}) \\ &\quad = \theta_g \log(2\theta_g \frac{\theta_g + \sqrt{\alpha_{n,g}}}{c_g \hat{d}_{n,g}^{-1}}) - (\theta_g + \sqrt{\alpha_{n,g}}). \end{aligned} \quad (42)$$

The first derivative of $U_{n,g}(\text{CP-1})$ w.r.t. c_g can be found as

$$\frac{\partial U_{n,g}(\text{CP-1})}{\partial c_g} = -\frac{2\theta_g \hat{d}_{n,g} \sqrt{\alpha_{n,g}} + 2\theta_g^2 \hat{d}_{n,g} - c_g}{2c_g \hat{d}_{n,g} (\sqrt{\alpha_{n,g}} + \theta_g)}. \quad (43)$$

The feasibility of CP-1 suggests that $\alpha_{n,g} = \theta_g^2 - c_g \hat{d}_{n,g}^{-1} \geq 0$, which implies that $2\theta_g^2 \hat{d}_{n,g} - c_g > 0$. Therefore, $\frac{\partial U_{n,g}(\text{CP-1})}{\partial c_g} < 0$, meaning that $U_{n,g}(\text{CP-1})$ is a decreasing function of c_g. Due to the monotonicity of $U_{n,g}(\text{CP-1})$ and because $c_g \in (0, \theta_g^2 \hat{d}_{n,g})$, we check the value of $U_{n,g}(\text{CP-1})$ when c_g approaches zero and when c_g approaches $\theta_g^2 \hat{d}_{n,g}$. Some algebraic manipulations reveal that $\lim_{c_g \to 0^+} U_{n,g}(\text{CP-1}) = +\infty$ and $\lim_{c_g \to \theta_g^2 \hat{d}_{n,g}} U_{n,g}(\text{CP-1}) = \theta_g(\log(2) - 1) < 0$ when c_g approaches $\theta_g^2 \hat{d}_{n,g}$.

The monotonicity of $U_{n,g}(\text{CP-1})$ and the boundary values of $U_{n,g}(\text{CP-1})$ for $c_g \in (0, \theta_g^2 \hat{d}_{n,g})$ suggests that there exists a unique point $\varrho_{n,g} \in (0, \theta_g^2 \hat{d}_{n,g})$ such that $U_{n,g}(\text{CP-1}) \geq 0$ for $c_g \in (0, \varrho_{n,g})$ and $U_{n,g}(\text{CP-1}) < 0$ for $c_g \in (\varrho_{n,g}, \theta_g^2 \hat{d}_{n,g})$. Moreover, the uniqueness of $\varrho_{n,g}$ suggests that we can find its value by applying the bisection methods within the interval $c_g \in (0, \theta_g^2 \hat{d}_{n,g})$.

Appendix F
Proof of Lemma 3

The derivative of $U_{n,g}$ w.r.t. $\hat{d}_{n,g}$ can be found as

$$\frac{\partial U_{n,g}(\text{CP-1})}{\partial \hat{d}_{n,g}} = \frac{2\theta_g \sqrt{\hat{d}_{n,g}} \cdot \sqrt{\theta_g^2 \hat{d}_{n,g} - c_g} + 2\theta_g^2 \hat{d}_{n,g} - c_g}{2\left(\sqrt{\theta_g^2 - c_g \hat{d}_{n,g}^{-1}} + \theta_g\right) \hat{d}_{n,g}^2} \quad (44)$$

which is greater than zero when $c_g < \theta_g^2 \hat{d}_{n,g}$, i.e., when CP-1 exists. This means that $U_{n,g}(\text{CP-1})$ is an increasing function of $\hat{d}_{n,g}$. Therefore, $\varrho_{n,g}$ is also an increasing function of $\hat{d}_{n,g}$ because $U_{n,g}(\text{CP-1}) = 0$ when $c_g = \varrho_{n,g}$ and $U_{n,g}(\text{CP-1})$ is an increasing function of $\hat{d}_{n,g}$. The lemma is proved by realizing that $\hat{d}_{n,g} = \frac{d_{n,g}}{4w_g}$.

References

[1] R. Kokku, R. Mahindra, H. Zhang, and S. Rangarajan, "NVS: A substrate for virtualizing wireless resources in cellular networks," *IEEE/ACM Trans. Netw.*, vol. 20, no. 5, pp. 1333–1346, Oct. 2012.

[2] T. L. Marzetta, "Noncooperative cellular wireless with unlimited numbers of base station antennas," *IEEE Trans. Wireless Commun.*, vol. 9, no. 11, pp. 3590–3600, Nov. 2010.

[3] H. Q. Ngo, E. G. Larsson, and T. L. Marzetta, "Energy and spectral efficiency of very large multiuser MIMO systems," *IEEE Trans. Commun.*, vol. 61, no. 4, pp. 1436–1449, Apr. 2013.

[4] G. Auer, O. Blume, and G. Auer, "Energy efficiency analysis of the reference systems, areas of improvements and target breakdown," Energy Aware Radio Netw. Technol., Tech. Rep. D2.3, 2010

[5] C. Jiang and L. J. Cimini, "Antenna selection for energy-efficient MIMO transmission," *IEEE Wireless Commun. Lett.*, vol. 1, no. 6, pp. 577–580, Dec. 2012.

[6] E. Björnson, L. Sanguinetti, J. Hoydis, and M. Debbah, "Optimal design of energy-efficient multi-user MIMO systems: Is massive MIMO the answer?" *IEEE Trans. Wireless Commun.*, vol. 14, no. 6, pp. 3059–3075, Jun. 2015.

[7] N. C. Luong, P. Wang, D. Niyato, Y.-C. Liang, F. Hou, and Z. Han. (2017). "Applications of economic and pricing models for resource management in 5G wireless networks: A survey." [Online]. Available: https://arxiv.org/abs/1710.04771

[8] J. Xu, L. Duan, and R. Zhang, "Energy group buying with loading sharing for green cellular networks," *IEEE J. Sel. Areas Commun.*, vol. 34, no. 4, pp. 786–799, Apr. 2016.
[9] V. Jumba, S. Parsaeefard, M. Derakhshani, and T. Le-Ngoc, "Resource provisioning in wireless virtualized networks via massive-MIMO," *IEEE Wireless Commun. Lett.*, vol. 4, no. 3, pp. 237–240, Jun. 2015.
[10] B. Colson, P. Marcotte, and G. Savard, "An overview of bilevel optimization," *Ann. Oper. Res.*, vol. 153, no. 1, pp. 235–256, Sep. 2007.
[11] C. Liang and F. R. Yu, "Wireless network virtualization: A survey, some research issues and challenges," *IEEE Commun. Surveys Tuts.*, vol. 17, no. 1, pp. 358–380, Mar. 2015.
[12] S. Abdelwahab, B. Hamdaoui, M. Guizani, and T. Znati, "Network function virtualization in 5G," *IEEE Commun. Mag.*, vol. 54, no. 4, pp. 84–91, Apr. 2016.
[13] S. Sun, L. Gong, B. Rong, and K. Lu, "An intelligent SDN framework for 5G heterogeneous networks," *IEEE Commun. Mag.*, vol. 53, no. 11, pp. 142–147, Nov. 2015.
[14] M. Zalghout, A. Khalil, M. Crussiere, S. Abdul-Nabi, and M. Hélard, "SDRAN-based user association and resource allocation in heterogeneous wireless networks," in *Proc. IEEE Wireless Commun. Netw. Conf. Workshops (WCNCW)*, Apr. 2016, pp. 296–302.
[15] A. Chang-Woo and C. Sang-Hwa, "SDN-based mobile data offloading scheme using a femtocell and WiFi networks," *Mobile Inf. Syst.*, vol. 2017, Feb. 2017, Art. no. 5308949.
[16] D. Zhang, Z. Chang, F. R. Yu, X. Chen, and T. Hämäläinen, "A double auction mechanism for virtual resource allocation in SDN-based cellular network," in *Proc. IEEE 27th Annu. Int. Symp. Pers., Indoor, Mobile Radio Commun. (PIMRC)*, Sep. 2016, pp. 1–6.
[17] M. Li, F. R. Yu, P. Si, E. Sun, Y. Zhang, and H. Yao, "Random access and virtual resource allocation in software-defined cellular networks with machine-to-machine communications," *IEEE Trans. Veh. Technol.*, vol. 66, no. 7, pp. 6399–6414, Jul. 2017.
[18] X. Xiong, L. Hou, K. Zheng, W. Xiang, M. S. Hossain, and S. M. M. Rahman, "SMDP-based radio resource allocation scheme in software-defined Internet of Things networks," *IEEE Sensors J.*, vol. 16, no. 20, pp. 7304–7314, Oct. 2016.
[19] Y. Cai, F. R. Yu, C. Liang, B. Sun, and Q. Yan, "Software-defined device-to-device (D2D) communications in virtual wireless networks with imperfect network state information (NSI)," *IEEE Trans. Veh. Technol.*, vol. 65, no. 9, pp. 7349–7360, Sep. 2016.
[20] G. Liu, F. R. Yu, H. Ji, and V. C. M. Leung, "Distributed resource allocation in virtualized full-duplex relaying networks," *IEEE Trans. Veh. Technol.*, vol. 65, no. 10, pp. 8444–8460, Oct. 2016.
[21] C. Liang, F. R. Yu, and X. Zhang, "Information-centric network function virtualization over 5G mobile wireless networks," *IEEE Netw.*, vol. 29, no. 3, pp. 68–74, May 2015.
[22] C. Liang, F. R. Yu, H. Yao, and Z. Han, "Virtual resource allocation in information-centric wireless networks with virtualization," *IEEE Trans. Veh. Technol.*, vol. 65, no. 12, pp. 9902–9914, Dec. 2016.
[23] K. Wang, F. R. Yu, and H. Li, "Information-centric virtualized cellular networks with device-to-device communications," *IEEE Trans. Veh. Technol.*, vol. 65, no. 11, pp. 9319–9329, Nov. 2016.
[24] Z. Chang, Z. Zhou, S. Zhou, T. Ristaniemi, and Z. Niu. (2016). "Towards service-oriented 5G: Virtualizing the networks for Everything-as-a-Service." [Online]. Available: https://arxiv.org/abs/1604.01739
[25] Z. Yin, F. R. Yu, S. Bu, and Z. Han, "Joint cloud and wireless networks operations in mobile cloud computing environments with telecom operator cloud," *IEEE Trans. Wireless Commun.*, vol. 14, no. 7, pp. 4020–4033, Jul. 2015.
[26] H. Zhang, Y. Xiao, S. Bu, D. Niyato, F. R. Yu, and Z. Han. (2017). "Computing resource allocation in three-tier IoT fog networks: A joint optimization approach combining Stackelberg game and matching." [Online]. Available: https://arxiv.org/abs/1701.03922
[27] R. Xie, F. R. Yu, H. Ji, and Y. Li, "Energy-efficient resource allocation for heterogeneous cognitive radio networks with femtocells," *IEEE Trans. Wireless Commun.*, vol. 11, no. 11, pp. 3910–3920, Nov. 2012.
[28] G. Liu, H. Ji, F. R. Yu, Y. Li, and R. Xie, "Energy-efficient resource allocation in full-duplex relaying networks," in *Proc. IEEE Int. Conf. Commun. (ICC)*, Jun. 2014, pp. 2400–2405.
[29] G. Liu, F. R. Yu, H. Ji, and V. C. M. Leung, "Energy-efficient resource allocation in shared full-duplex relaying cellular networks," in *Proc. IEEE Global Commun. Conf. (GLOBECOM)*, Dec. 2014, pp. 2631–2636.
[30] G. Liu, F. R. Yu, H. Ji, and V. C. M. Leung, "Virtual resource management in green cellular networks with shared full-duplex relaying and wireless virtualization: A game-based approach," *IEEE Trans. Veh. Technol.*, vol. 65, no. 9, pp. 7529–7542, Sep. 2016.
[31] D. Niyato, F. Adachi, P. Wang, and D. I. Kim, "Competitive cell association and antenna allocation in 5G massive MIMO networks," in *Proc. IEEE Int. Conf. Commun. (ICC)*, Jun. 2015, pp. 3867–3872.
[32] K. Zhu and E. Hossain, "Virtualization of 5G cellular networks as a hierarchical combinatorial auction," *IEEE Trans. Mobile Comput.*, vol. 15, no. 10, pp. 2640–2654, Oct. 2016.
[33] Z. Chang, Z. Han, and T. Ristaniemi, "Energy efficient optimization for wireless virtualized small cell networks with large-scale multiple antenna," *IEEE Trans. Commun.*, vol. 65, no. 4, pp. 1696–1707, Apr. 2017.
[34] H. Yang and T. L. Marzetta, "Performance of conjugate and zero-forcing beamforming in large-scale antenna systems," *IEEE J. Sel. Areas Commun.*, vol. 31, no. 2, pp. 172–179, Feb. 2013.
[35] S. Li and J. Huang, "Price differentiation for communication networks," *IEEE/ACM Trans. Netw.*, vol. 22, no. 3, pp. 703–716, Jun. 2014.
[36] L. Duan, J. Huang, and B. Shou, "Duopoly competition in dynamic spectrum leasing and pricing," *IEEE Trans. Mobile Comput.*, vol. 11, no. 11, pp. 1706–1719, Nov. 2012.
[37] P. Belotti, C. Kirches, S. Leyffer, J. Linderoth, J. Luedtke, and A. Mahajan, "Mixed-integer nonlinear optimization," *Acta Numer.*, vol. 22, pp. 1–131, May 2013.
[38] G. Pataki, M. Tural, and E. B. Wong, "Basis reduction and the complexity of branch-and-bound," in *Proc. 21st Annu. ACM-SIAM Symp. Discrete Algorithms (SODA)*, 2010, pp. 1254–1261.
[39] M. Chiang, *Geometric Programming for Communication Systems*, vol. 2. Hanover, MA, USA: Now, Jul. 2005.
[40] G. Xu, "Global optimization of signomial geometric programming problems," *Eur. J. Oper. Res.*, vol. 233, no. 3, pp. 500–510, 2014.
[41] S. Boyd and L. Vandenberghe, *Convex Optimization*. New York, NY, USA: Cambridge Univ. Press, 2004.
[42] G. B. Thomas, M. D. Weir, J. R. Hass, and F. R. Giordano, *Thomas' Calculus*, 11th ed. Boston, MA, USA: Addison-Wesley, 2005.

Ye Liu received the B.Eng. degree (Hons.) in electronic and communication engineering and the Ph.D. degree in electronic engineering from the City University of Hong Kong, Hong Kong, in 2009 and 2014, respectively. He was a Visiting Student at the Laboratory of Information, Networking and Communication Sciences, Paris, France. He was also an Intern at Nokia Bell Labs, France, and was a Post-Doctoral Research Associate with the Wolfson School of Mechanical, Electrical and Manufacturing Engineering, Loughborough University, U.K. He is currently a Post-Doctoral Research Assistant with the Department of Engineering Science, University of Oxford. His research interests include index modulation, non-orthogonal multiple access, resource allocation, and network coding.

Mahsa Derakhshani (S'10–M'13) received the B.Sc. and M.Sc. degrees from the Sharif University of Technology, Tehran, Iran, in 2006 and 2008, respectively, and the Ph.D. degree from McGill University, Montréal, QC, Canada, in 2013, all in electrical engineering. From 2013 to 2015, she was a Post-Doctoral Research Fellow with the Department of Electrical and Computer Engineering, University of Toronto, Toronto, ON, Canada, and a Research Assistant with the Department of Electrical and Computer Engineering, McGill University. From 2015 to 2016, she was an Honorary NSERC Post-Doctoral Fellow with the Department of Electrical and Electronic Engineering, Imperial College London. She is currently a Lecturer (Assistant Professor) in digital communications with the Wolfson School of Mechanical, Electrical and Manufacturing Engineering, Loughborough University. Her research interests include radio resource management for wireless networks, software-defined wireless networking, applications of convex optimization and game theory for communication systems, and spectrum sensing techniques in cognitive radio networks. Dr. Derakhshani received the John Bonsall Porter Prize, the McGill Engineering Doctoral Award, and the Fonds de Recherche du Que?bec–Nature et Technologies and Natural Sciences and Engineering Research Council of Canada Postdoctoral Fellowships. She currently serves as an Associate Editor of the *IET Signal Processing Journal*.

Saeedeh Parsaeefard (S'09–M'14) received the B.Sc. and M.Sc. degrees from Amirkabir University of Technology (Tehran Polytechnic), Tehran, Iran, in 2003 and 2006, respectively, and the Ph.D. degree in electrical and computer engineering from Tarbiat Modares University, Tehran, in 2012. She was a Post-Doctoral Research Fellow with the Telecommunication and Signal Processing Laboratory, Department of Electrical and Computer Engineering, McGill University, Montreal, QC, Canada. From 2010 to 2011, she was a Visiting Ph.D. Student with the Department of Electrical Engineering, University of California at Los Angeles, Los Angeles, CA, USA. She is currently a Research Assistant with the Department of Electrical and Computer Engineering, McGill University, and a Faculty Member with the Iran Telecommunication Research Center. Her current research interests include resource management in software-defined networking, Internet of Things and the fifth generation of wireless networks as well as applications of robust optimization theory, and game theory on the resource allocation and management in wireless networks. She received the IEEE Iran Section Women in Engineering Awards in 2018.

Sangarapillai Lambotharan (SM'06) received the Ph.D. degree in signal processing from Imperial College London, U.K., in 1997. He was a Post-Doctoral Research Associate with Imperial College London until 1999. He was a Visiting Scientist at the Engineering and Theory Centre, Cornell University, Ithaca, NY, USA, in 1996. From 1999 to 2002, he was with the Motorola Applied Research Group, U.K., and investigated various projects, including physical link layer modelling and performance characterization of GPRS, EGPRS, and UTRAN. He was with King's College London and Cardiff University as a Lecturer and a Senior Lecturer, respectively, from 2002 to 2007. He is currently a Professor of digital communications and the Head of the Signal Processing and Networks Research Group, Wolfson School Mechanical, Electrical and Manufacturing Engineering, Loughborough University, U.K. His current research interests include 5G networks, MIMO, radars, smart grids, machine learning, network security, and convex optimizations and game theory. He has authored or co-authored approximately 200 technical journal and conference articles in these areas.

Kai-Kit Wong (M'01–SM'08–F'16) received the B.Eng., M.Phil., and Ph.D. degrees in electrical and electronic engineering from the Hong Kong University of Science and Technology, Hong Kong, in 1996, 1998, and 2001, respectively.

After graduation, he took up academic and research positions at the University of Hong Kong, Lucent Technologies, Bell-Labs, Holmdel, NJ, USA, the Smart Antennas Research Group, Stanford University, and the University of Hull, U.K. He is the Chair in wireless communications at the Department of Electronic and Electrical Engineering, University College London, U.K. His current research centers around 5G and beyond mobile communications, including topics such as massive MIMO, full-duplex communications, millimeter-wave communications, edge caching and fog networking, physical layer security, wireless power transfer and mobile computing, V2X communications, and of course cognitive radios. There are also a few other unconventional research topics that he has set his heart on, including for example, fluid antenna communications systems, remote ECG detection, and so on.

Dr. Wong is a fellow of IET. He was a co-recipient of the 2013 IEEE Signal Processing Letters Best Paper Award and the 2000 IEEE VTS Japan Chapter Award at the IEEE Vehicular Technology Conference in Japan in 2000, and a few other international best paper awards. He is also on the editorial board of several international journals. He has served as a Senior Editor for the IEEE COMMUNICATIONS LETTERS since 2012 and also for the IEEE WIRELESS COMMUNICATIONS LETTERS since 2016. He had also previously served as an Associate Editor for the IEEE SIGNAL PROCESSING LETTERS from 2009 to 2012 and an Editor for the IEEE TRANSACTIONS ON WIRELESS COMMUNICATIONS from 2005 to 2011. He was also a Guest Editor of the IEEE JSAC SI on virtual MIMO in 2013 and currently a Guest Editor of the IEEE JSAC SI on physical layer security for 5G.